I give permission for public access to my thesis and for copying to be done at the discretion of the archives' librarian and/or the College library.

_____ _____

Signature Date

IDENTIFICATION OF RESIDUES OF THE *PLASMODIUM FALCIPARUM* VARIANT ANTIGEN PROTEIN PfEMP1 THAT ARE INVOLVED IN BINDING ICAM-1

by

Jennifer Reagan

A Paper Presented to the

Faculty of Mount Holyoke College in

Partial Fulfillment of the Requirements for

the Degree of Bachelors of Arts with

Honor

Department of Biological Sciences

South Hadley, MA 01075

May, 2006

This paper was prepared
under the direction of
Professor Amy Springer
for eight credits.

DEDICATION

I dedicate this paper to my parents.

They have helped me through so much

and without them my education

would not have been possible.

AKNOWLEDGEMENTS

I would like to thank my advisor Amy Springer. You have helped me so much both on this project and in other areas of my life. I think you will be a great teacher and I wish you all the best of luck.

I would also like to thank my lab buddies: Noel, Julie, and Tolu. Thank you for keeping me company through some long days and sympathizing with me when everything seemed to be going wrong.

Thanks to my committee members Rachel Fink and Jennifer Van Wijngaarden. Both of your classes taught me so much and you are both such wonderful people.

I would also like to thank Marian Rice. Thank you for being patient with me, and giving a crash course in how to use a fluorescent microscope.

Last but not least I would like to thank Jeff Knight and the rest of the biology department for being so understanding, and kind. You all have helped make my experience at Mount Holyoke rewarding and enlightening.

TABLE OF CONTENTS

LIST OF FIGURES

LIST OF TABLES

ABSTRACT

Plasmodium falciparum is the parasite responsible for causing most cases of malaria. While the pathogenesis of the disease is variable, severe malaria is often associated with the sequestration of parasite infected erythrocytes (IE's) in various organs of the body. The sequestration of IE's is due to adhesion molecules called *Plasmodium falciparum* erythrocyte membrane protein 1 (PfEMP1) on the surface of IE's. PfEMP1 adheres to various host receptors on the surfaces of the endothelial cells in various tissues. ICAM-1 is the receptor in the brain that is believed to be responsible for the sequestering of IE's which is associated with the disease cerebral malaria.

In this paper, threonine (aa837), glutamate (aa834), and lysine (aa831) of the DBL2βC2 region of the PfEMP1 A4tres, were converted to alanine using site specific mutagenesis. These residues were chosen using a comparative modeling program that formed a plausible 3D structure of the DBL2βC2 region. Binding / Immunofluorescence assays were performed to characterize ICAM-1 binding in each mutant. The results of these assays showed that lysine was probably not involved in binding ICAM-1 while threonine may be involved in ICAM-1 binding. Also, changing glutamate to alanine increased binding suggesting that it is of structural significance.

INTRODUCTION

Malaria, the most debilitating of all parasitic diseases, is caused by the *Plasmodium* protozoan. There are four *Plasmodium* species known to cause disease in humans: *P. falciparum*, *P. vivax*, *P. ovale*, and *P. malariae*. Of these four species *P. falciparum* is the most pathogenic, with *P. vivax* to a lesser extent (Miller et al., 2002). Globally *P. falciparum* is responsible for about 2 million deaths and more than 500 million clinical cases of malaria annually (Snow et al., 2005). In Africa alone, at least a 1 million deaths and more than 200 million clinical cases of malaria are attributed to *P. falciparum* yearly (Snow et al., 1999).

Currently forty-one percent of the world's population lives in areas where malaria is transmitted, which includes most of Sub-Saharan Africa and South Asia (CDC, 2004). These areas provide the optimum environment for the *Anopheles* mosquito, which is the vector through which the *Plasmodium* parasite is transmitted (Snow et al., 1999). The major transmitter of *P. falciparum* among African populations is *Anopheles gambiae*.

Historically, malaria was widespread throughout temperate North America and Europe, but by the mid-twentieth century malaria had been eradicated in most of these regions (Figure 1). However, *A. quadrimaculatus* and *A. freeborni,* the mosquitoes in North America responsible for transmitting malaria are still abundant (CDC, 2004). Therefore, there is a possibility that malaria could be reintroduced.

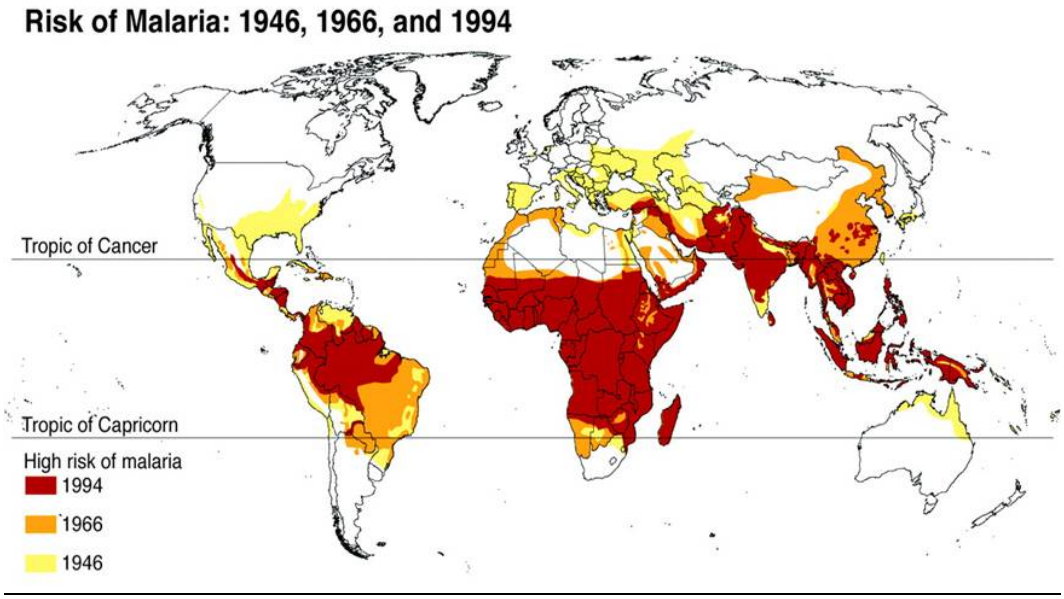

Figure 1- Regions affected by malaria from 1946 -1994 (Sachs, 2002)

Life Cycle of *Plasmodium*

The *Plasmodium* life cycle is very intricate, including a liver stage, blood stage, and mosquito stage (Figure 2). Initially *Plasmodium* sporozoites are transmitted to a person by a mosquito bite. Specifically, sporozoites are contained within the female mosquito's saliva, and a very few are injected into the subcutaneous tissue. Once in the bloodstream, sporozoites are carried to the liver. There they pass through several hepatocytes, until receptors on their surface adhere with heparin sulfate proteoglycans (Weatherall et al., 2002). After sporozoites invade the liver cells, there is a period of development that lasts 7-10 days. This time is not associated with symptoms of the disease, but is a time of cell division that culminates in the release of 20,000-40,000 merozoites. Since infection is initiated with only a few sporozoites, this period is essential for the progression of the disease and is a prime target for possible anti-malaria drugs (Smith et al., 2004).

Released merozoites travel through the bloodstream, and adhere to host erythrocytes through a set of adhesion proteins. They then invade the cell by inducing a vacuole in the cell membrane, and entering by formation of a moving junction. Once a merozoite invades an erythrocyte, it undergoes a cycle of asexual division which lasts approximately 48 hours, and can release from 10-24 new merozoites into the vascular system once completed. The erythrocyte stage of the *Plasmodium* lifecycle is responsible for the pathology of malaria. The use of

intracellular replication by *Plasmodium* as well antigenic variation reduces the host's ability to eradicate parasites. In some individuals, a chronic infection is produced that can last over a year (Smith et al., 2004).

In a number of erythrocytes, the merozoites differentiate into male or female gametocytes which are the sexual form of the parasite. *P. vivax* produces gametocytes before the symptomatic stage of the disease, while *P. falciparum* produces its gametocytes much later on (Miller et al., 2002). Currently it is unknown why some merozoites differentiate into gametocytes, while others do not. The life cycle is completed when gametocytes infect female mosquitoes, and undergo sexual reproduction in the gut of the mosquito to produce sporozoites.

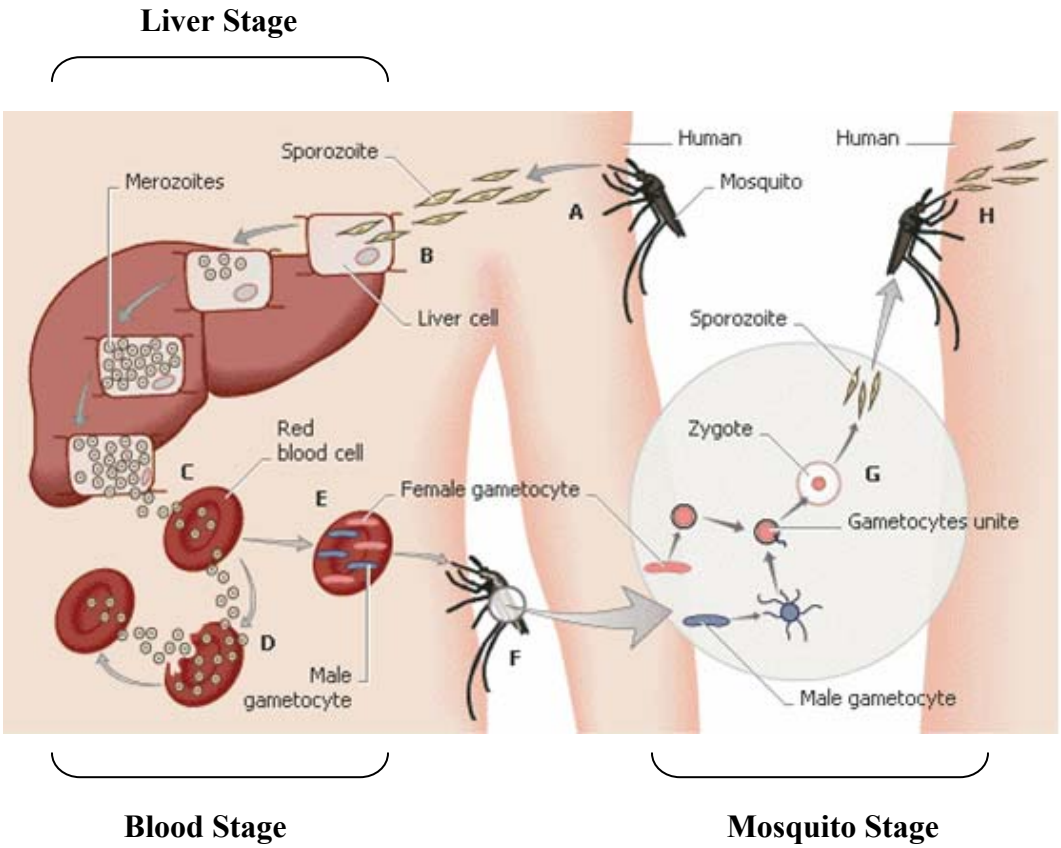

Figure 2- Schematic diagram of the various life cycle stages of *Plasmodium falciparum* (http://images.encarta.msn.com/xrefmedia/aer, © Microsoft)

Pathology of Malaria

The pathogenesis of malaria can range in severity, with severe malaria affecting multiple systems and organs. Malaria is generally divided into two types mild or severe. Classic symptoms of mild malaria include fever, chills, sweating, and muscle pains. Patients with severe malaria sometimes exhibit anemia, kidney failure, respiratory distress, and cerebral malaria (Weatherall et al., 2002).

Many symptoms of malaria are highly interconnected. For example, respiratory distress is believed to be due metabolic acidosis (Miller et al., 2002). Metabolic acidosis is a condition when the blood pH becomes too low (< 7.35), and seems to be due to a combination of several factors that reduce oxygen delivery. First, the destruction of erythrocytes causes anemia, which reduces the overall ability of blood to transport oxygen. Second, the parasites produce lactic acid. In severe cases, the abundance of lactic acid can lower the blood pH, leading to a reduced ability of the blood cells to bind oxygen. Third, the sequestering of erythrocytes in specific tissues can reduce blood flow, which subsequently reduces oxygen transport (Miller et al., 2002). This is just one example that shows that a single symptom may be due to one or several processes, making the treatment of malaria difficult. Therefore, the most hopeful treatment of malaria is through either control of the *Anopheles* mosquito population, or through the development of a vaccine.

Sequestering and the Role of PfEMP1

Severe malaria is often associated with the sequestration of parasite infected erythrocytes (IE's) in various organs of the body. The sequestering of IE's is thought to have evolved in order for the parasites to avoid clearance by the spleen, since non-adherent IE's are rapidly cleared by the spleen (Smith et al., 2004). Only *Plasmodium falciparum* and none of the other *Plasmodium sp.* that infect humans uses this mechanism of sequestration (Pongponratin et al., 1991). Since *Plasmodium falciparum* is also the most pathogenic of the *Plasmodium sp*., this is evidence to support the link between sequestration and pathogenicity of disease.

The sequestration of IE's is due to adhesion molecules that the parasites place on the surface of the membrane. These adhesion molecules are called *Plasmodium falciparum* erythrocyte membrane protein 1 (PfEMP1). PfEMP1 are variant antigen proteins encoded by *var* genes. There are approximately 50 different *var* genes that vary between different *Plasmodium falciparum* strains (Su et al., 1995). A strain is a genetic variant or subpopulation, while a line is a cloned descendent of a single cell. An example of a commonly used clonal line is A4 (Smith et al., 1998). The A4 clone was derived by clonal dilution of ICAM-1 binding IE's infected with *Plasmodium falciparum* strain IT 4/25/5 (Smith, Craig et al., 2000). For the purpose of this study, the name of a clonal line indicates the specific PfEMP1 expressed in this line. Many lines of IT 4/25/5 have been made including IT-ICAM, A4tres, and FCRvarCSA. The line expressing A4tres is able

to bind ICAM-1 more strongly than the A4 line. A4tres was derived from A4 by treating A4 with trypsin to remove part of the protein and selecting IE's that were able to bind ICAM-1 (Smith, Craig et al., 2000). The part of the protein that was removed somehow revealed the ICAM-1 binding region. Currently, the physiological significance of the trypsin dependence of this binding region is not understood.

The PfEMP-1 molecules are glycoproteins that adhere to various host receptors on the surfaces of the endothelial cells in the microvasculature, brain, placenta, and other organs. The most characterized host receptor molecules are CD36, CSA (Chondroitin Sulfate A), and ICAM-1 (Intercellular Adhesion Molecule – 1).

CD36 has been associated with microvascular adhesion of IE's (Barnwell et al., 1989). CD36 is an 88 kDa integral membrane glycoprotein that is found on the surface of endothelial cells, platelets, and monocytes (Greenwalt et al., 1992). Besides being a receptor for *Plasmodium falciparum* IE's, it has been shown to play many roles in the body including: a platelet collagen receptor, a possible receptor of thrombospondin (TSP) to mediate the TSP-dependent adhesion of monocytes to macrophages, and platelets, and may participate in signal transduction in the activation of platelets (Greenwalt et al., 1992). While CD36 has not been proven to cause the sequestration of IE's *in vivo*, many different *in vitro* experiments have been performed that suggest CD36 is a receptor for IE's. Ockenhouse et al. (1989) found that IE's bound to CD36 which was immobilized

on plastic beads. They further supported their findings when they showed that in fluid phase assays ^{125}I-labeled CD36 also bound IE's.

CSA is probably the best characterized receptor of IE's and has been associated with placental malaria (Rogerson et al., 1995). CSA is a glycosaminoglycan composed of N-acetyl-galactosamine and glucouronic acid, and is sulfated mainly at carbon 4 of the repeating disaccharide. It is commonly found as part of a proteoglycan, and is a major structural component of the extracellular matrix and cartilage. In placental malaria, large amounts of IE's sequester in the maternal circulation of the placenta. When IE's were taken from women with placental malaria they not only bound to purified CSA, but the binding of these IE's to freshly frozen sections of human placenta was competitively inhibited by CSA (Fried et al., 1996).

During the first pregnancy, women contract placental malaria even though they often have clinical immunity to other forms of malaria. This is due to the fact that the PfEMP1's that are involved in placental malaria are a subset of PfEMP1's that bind CSA but do not seem to bind to other receptors such as CD36, for which they have already acquired antibodies (Kraemer et al., 2003). An example of one such PfEMP1 is FCRvarCSA, which binds to CSA but not CD36 or ICAM-1 (Buffet et al., 1999). After several pregnancies women in endemic areas begin to produce antibodies that block CSA binding to IE's (Fried et al., 1998).

All of the above is evidence to the fact that IE's sequester at specific receptors, but it is still not understood why malaria causes sequestration in some individuals but not others.

ICAM-1

ICAM-1 is believed to be the primary host receptor molecule linked to cerebral malaria (Weatherall et al., 2002). ICAM-1 is a 90–115 kDa glycoprotein that is found in endothelial cells, including brain, and hematopoietic cells (Chakravorty et al., 2005). ICAM-1 is a member of the immunoglobulin-like (Ig-like) superfamily, and is comprised of five different extracellular Ig-like domains (Chakravorty et al., 2005). It also contains a transmembrane domain, and a cytoplasmic tail (Stolpe et al., 1996).

In the body, ICAM-1 exists in membrane bound form as well as in soluble form, which comes from ICAM1-1 that has been cleaved from the surface of cells through proteolytic cleavage. ICAM-1 functions as a receptor for several molecules including leukocyte function associated molecule-1 (LFA-1), and the human rhinovirus (HRV) (figure 3). ICAM-1/LFA-1 interaction plays a role in leukocyte recruitment and subsequent cell-cell adhesion reactions (Piela-Smith et al., 1991). Endothelially expressed ICAM-1 is up-regulated in response to many inflammatory mediators (Chakravorty et al., 2005).

There is much evidence to support the idea that ICAM-1 is involved in the pathogenesis of severe malaria. First, ICAM-1 is up-regulated in response to inflammation, and is thought to be up-regulated in brain in response to *P. falciparum* infection (Turner et al., 1998). It is believed that this up-regulation may increase sequestration of IE's in the brain, which would contribute to the pathogenesis of the disease (Chakravorty et al., 2005). Second, in one study autopsy samples taken from people that died of cerebral malaria showed that brain vessels with sequestered parasites also contained ICAM-1 (Turner et al., 1994). Third, severe disease is also commonly seen in people that produce ICAM-1 that contains a genetic polymorphism in the Ig-like N-terminal domain (Fernandez-Reyes et al., 1997). People who are homozygous for this mutation have an increased susceptibility to cerebral malaria, which shows a correlation between ICAM-1 and severity of malaria (Fernandez-Reyes et al., 1997). Fourth, adhesion of IE's to ICAM-1 was higher in isolates from patients with clinical malaria than in parasitized community controls and tended to be higher in those with cerebral malaria than in controls (Newbold et al., 1997). These results agree with and support the finding that ICAM-1 is up-regulated during *Plasmodium falciparum* infection.

Tse et al. (2004) characterized the PfEMP1 binding region of ICAM-1 under both static and flow conditions. Based on previous studies that suggested the ICAM-1 binding region for IE's was near the BE and D beta sheet 'side' of the molecule, these authors chose amino acid residues G14-L30 and K39-K50 for

alanine substitution. Their assays were performed on 3 different parasite lines A4, IT-ICAM, and JDP8. A4 has a low avidity for ICAM-1, while IT-ICAM and JDP8 are high avidity binders. Interestingly IT-ICAM and JDP8 share common amino acids that are important for binding. Figure 4 is a summary of their results.

Tse et al., (2004) found that in JDP8 and IT-ICAM, under static conditions, cysteine 21, and serine 22 were involved in binding, while in A4 lysine 29 was particularly important. All lines also require amino acids Glycine 14- leucine18, and leucine 42-44 for maximum binding of IE's. Under flow conditions, an alanine substitution to these previously mentioned amino acids usually caused a greater decrease in binding. Also, threonine 20, cysteine 21, lysine 39, lysine 40, asparagine 47, and lysine 50 were shown to decrease the binding of IE's to ICAM (figure 3).

The similarities between the lines with the exception of lysine 29, implies that the binding interaction between ICAM-1 and PfEMP1 has a similar mechanism across variants (Tse et al., 2004). These results also hint at a possible common evolutionary origin of ICAM-1 binding in PfEMP1 (Tse et al., 2004).

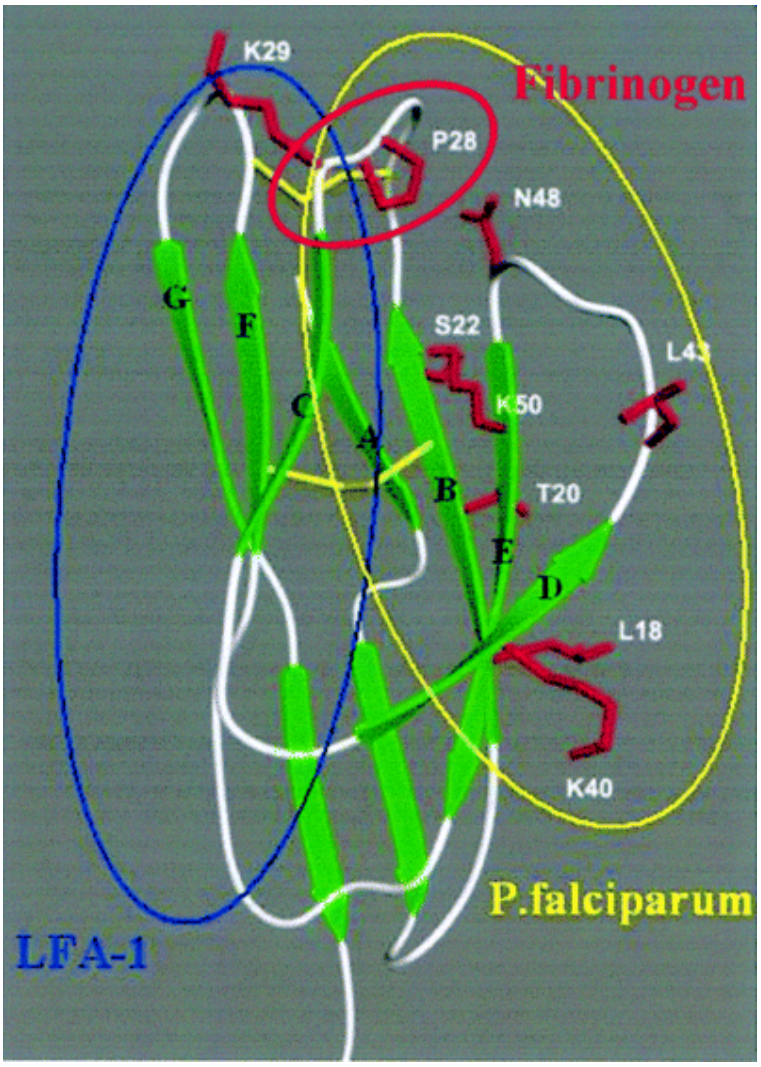

Figure 3- Diagram showing a representation of the crystal structure of the N-terminal Ig-like domain of ICAM-1 where the circles designate proposed areas of binding by LFA-1 (blue circle), fibrinogen (red circle) and *P. falciparum* (yellow circle). The binding of rhinovirus to ICAM-1 involves residues over the whole domain. Notice that the proposed binding domains of LFA-1, and *P. falciparum* overlap (Tse et al., 2004).

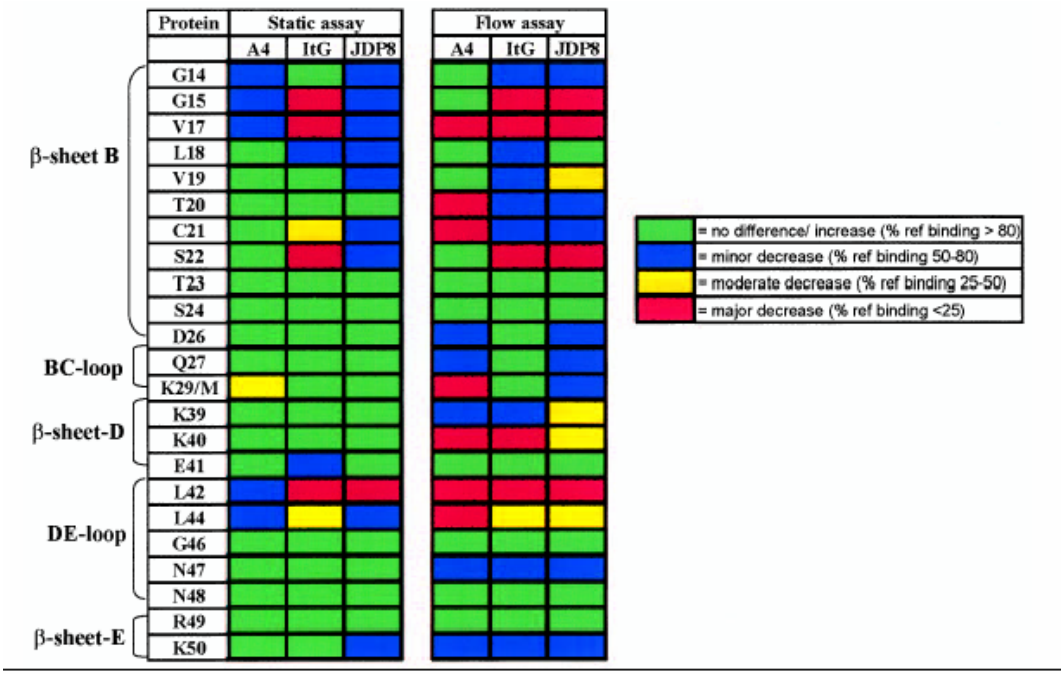

Figure 4- Summary of results found by Tse et al., (2004). The static assay tested the ability of the different lines of PfEMP1 (ItG = IT-ICAM, A4, JDP8) to bind the mutant ICAM-1 without movement while the flow assay tried to simulate the current of blood in the circulatory system. The residues that were substituted with alanine in each mutant are shown in the protein column using one letter amino acid code. The 3D structures where these residues are found appear at the left of the diagram. The stated increases and decreases are relative to normal ICAM-1/PfEMP1 binding.

Structure of PfEMP1

PfEMP1 are a family of variant antigens encoded by *var* genes. An organism that displays antigenic variation has the ability to change the glycoproteins on the surface of the organism that the immune system uses to form antibodies. Variant antigens are often placed on the surface of IE's or on the surface of parasites as in trypanosomes to evade the immune system. While many organisms use variant antigens to fool the immune system, *P. falciparum* also uses these proteins to bind to the endothelial tissue. The fact that these variant antigens have specific functions suggests that they must retain a certain degree of similarity in order to function as binding proteins (Chattopadhyay et al., 2003). Only one variant is displayed on the surface of IE's at a time, and the number of asexual lifecycles that display the same variant can vary. However, these proteins can be changed relatively quickly, which causes waves of parasitism (Kyes et al., 2001). Most of the parasites are expressing the same PfEMP1 at any given point in time during the course of an infection. As the body begins to produce antibodies to one PfEMP1 and destroy the parasite, new generations of the parasite will begin to express a different PfEMP1.

How this action is coordinated and which signals are involved is unknown. Recent work into the rates of transition on and off in clonal expression of PfEMP1 have found that rates of transition on and off are highly variable between different variants and among a given variant (Horrocks et al., 2004). However, on and off

rates are constant for genetically identical clones expressing the same *var* gene suggesting that these rates are an intrinsic property of each gene (Horrocks et al., 2004).

PfEMP1 are encoded by genes consisting of two exons (Figure 5). The first exon of a *var* gene codes for the extracellular binding region and transmembrane region, while the second codes for a highly conserved cytoplasmic tail (Smith et al., 2001). The extracellular binding domain is mainly composed of the N-terminal segment (NTS), and combinations of c2 domains, cysteine-rich interdomain regions (CIDR), and Duffy binding like domains (DBL) (Smith, Subramanian et al., 2000). DBL domains can be broken down into 5 subgroups (α,β,γ,δ, and ε), while CIDR domains have 3 subgroups (α,β,γ) based on their homology (Smith et al., 2001). CIDRα domains have been implicated in CD36 binding (Baruch et al., 1997), DBLγ domains to CSA (Rogerson et al., 1995), and DBLβ domains to ICAM-1 (Smith, Craig et al., 2000).

However, many domains may be present on a single PfEMP1 protein, and it may be able to bind to multiple host receptors through different domains. Also, the order of these domains is not random and it has been shown that certain combinations of domains preferentially occur. An example of this is the preferred association of the DBL2βc2 tandem that has been shown to bind ICAM-1 (Smith, Subramanian et al., 2000). Another preferred association is seen between DBL5δ and CIDR2β. Also there is a semi-conserved head structure in PfEMP1 which is composed of DBL1α and CIDRα (Smith et al., 2001).

Both the DBL2β and c2 domain are necessary for proper binding of ICAM-1 (Springer et al., 2004, Smith, Subramanian et al., 2000)(Figure 5 & 6). They found a likely ICAM-1 binding region of the DBL2βc2 tandem of the PfEMP1 A4tres through truncation analysis. When truncation was performed on the N-terminal side of DBL2βc2, it was found that if the protein was truncated to the tryptophan (W) at amino acid position 829, ICAM-1 binding would decrease to 51.6%. However, it is important to note that the W residue is only 19 amino acids from the N-terminus of the DBL2β domain, which will be denoted as N-19. If the protein was deleted to the conserved cysteine C4 at amino acid position N-42, no ICAM-1 was bound. Also, when C-terminal truncation was performed on the C-terminal side of DBL2βc2, it was found that if the C-terminal end to the C-71 amino acid position was deleted, ICAM-1 binding would still bind. However if the c2 was truncated to the C-99 amino acid position ICAM-1 binding was completely lost. Therefore the important ICAM-1 binding regions of DBL2βc2 are from the N-19 to the N-42 amino acid (C4), and from the C-terminus to the C-99 amino acid.

Moreover, to further characterize the DBL2βc2 region, Springer et al. (2004) made chimeras of different DBL2β and c2 domains. Chimeras were constructed that combined the binding A4tres DBL2β region with non-binding C-terminus regions from FCR3varCSA DBL2βc2. Other chimeras were made that combined the binding C-terminus regions from IT-ICAM DBL2βc2 with the binding A4tres

DBL2β region. Recall that IT-ICAM is a line of PfEMP1 that binds ICAM-1, while FCR3varCSA is a line of PfEMP1 that does not bind ICAM-1.

Only three chimeras were still able to bind ICAM. The first two chimeras contained an N-terminal DBL2β region and C-terminal c2 region of A4tres with just the C7 DBL region swapped with the same regions from either FCR3varCSA or It-CAM. C7 DBL region is region of the DBL2βc2 domains that lies between the conserved cysteine C7 of the DBL2β and the N-terminus of the c2. The result of these chimeras suggests that the C7 DBL region is not necessary for binding. The third functional chimera was an A4tres DBL2βc2 with the last half of the C-terminus replaced by the homologous region of IT-ICAM. Unexpectedly, the entire c2 region of A4tres could be replaced by a c2 from another ICAM binder, IT-ICAM. However, if the first half of the c2 region was replaced by IT-ICAM, ICAM-1 would not bind. This suggests that there are functional interactions between the DBL2β and c2 region (Springer et al., 2004).

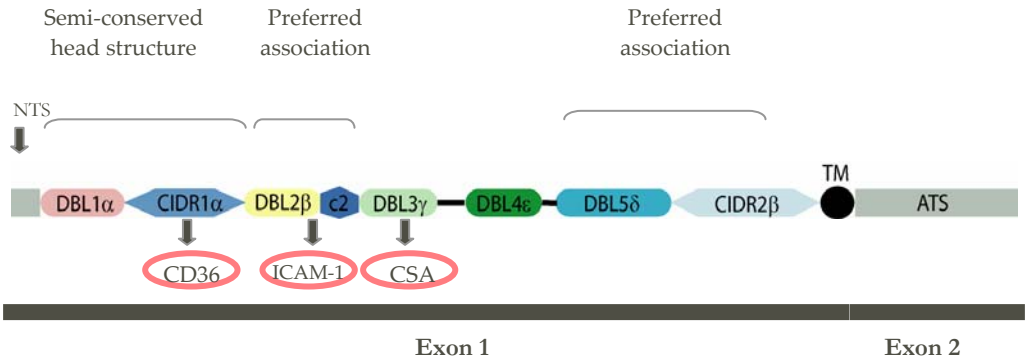

Figure 5- Structure of a typical PfEMP1 displaying preferred binding domains, and the position those domains relative to the exons which encode them (Smith et al., 2001). TM is the transmembrane region. NTS is the N-terminal segment. ATS is the highly conserved acidic terminal segment otherwise known as the cytoplasmic tail. Domains shown to have ability to bind CD36, ICAM-1 or CSA are indicated.

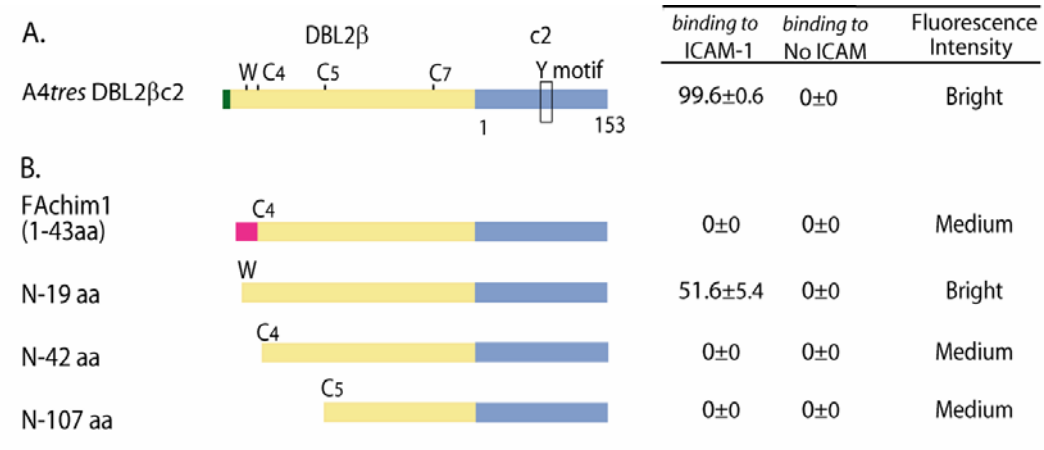

Figure 6- Ability of the DBL2βc2 to bind ICAM-1 after truncation of areas of the DBL2β region (Springer et al., 2004). The A4tres DBL2βc2 is shown at top, the DBL2β in yellow and the c2 in blue. W is the conserved tryptophan, while C4, C5, and C7 are conserved cysteines. The Y motif is conserved in most c2 sequences, but not in FCR3varCSA. N-xx aa denotes N terminal end minus number of amino acids. The fluorescence is reported relative to the amount of DBL2βc2 expressed on the surface of the COS-7 cells: the brighter fluorescence, greater the amount of PfEMP1. The "binding to No ICAM" column shows that cells expressing PfEMP1 didn't bind to beads with no ICAM-1, while the "binding to ICAM" column shows the percentage of cells expressing PfEMP1 that were binding beads.

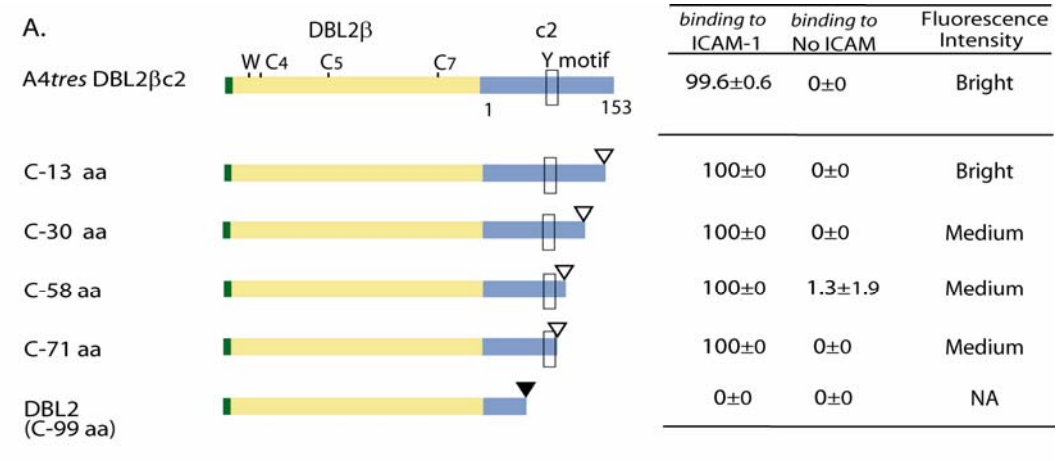

Figure 7- Ability of the DBL2βc2 to bind ICAM-1 after truncation of areas of the c2 region (Springer et al., 2004). A4tres DBL2βc2 shown at top as in figure 6. C-xx aa denotes C terminal end minus xx amino acids. See figure 6 for label descriptions.

DBL Crystal Structures

The CIDR domain is unique to PfEMP1, but the DBL domain was originally identified in another family of *Plasmodium* proteins, erythrocyte binding-like (EBL). EBL are a family of invasion proteins, which characteristically have at least one DBL domain, a transmembrane region, and a cysteine-rich C-terminal region (Adams et al., 1992). Erythrocyte binding antigen-175 (EBA-175) is a member of the EBL family.

In both invasion and sequestration, *Plasmodium falciparum* targets glycosylated host cells by expressing ligands such as EBA-175, which bind to sugar residues (Waters et al., 2005). EBA-175 binds a heavily sialylated glycoprotein called glycophorin A (GpA) (Waters et al., 2005). GpA is common surface protein on erythrocytes. In this transmembrane dimer, the N-terminus of each GpA monomer that is exposed on the extracellular surface (Tolia et al., 2005). The 2 DBL domains of EBA-175 are responsible for erythrocyte binding. Individually the domains are designated F1 and F2 respectively, while collectively the tandem is known as RII.

Recently, the crystal structure of the EBA-175 DBL domains (RII) has been described to a 2.3 Å resolution (Tolia et al., 2005). A crystal structure of EBA-175 RII was made for both RII alone and RII bound to a glycan. Tolia et al. (2005) cocrystallized the RII with α-2,3-sialyllactose to simulate the binding interactions found between the RII and erythrocytes. They found that the 6

glycan binding sites were formed by the dimerization of the two DBL domains, and all of them were at the dimer interface (Tolia et al., 2005). The binding sites and the residues found to be involved in binding can be seen in Figure 8. Tolia et al. (2005) tested the ability of these binding sites to bind erythrocytes after important residues were modified by point mutations. When residues involved in dimeric interactions were modified, erythrocyte binding decreased suggesting that dimerization is vital for optimum erythrocyte binding (Tolia et al., 2005). Also when residues involved in glycan binding were changed (usually to alanine), erythrocyte binding lessened, which shows that all six glycan binding sites are involved in binding erythrocytes (Tolia et al., 2005).

Since the DBL domains of EBA-175 share a great degree of homology with the DBL2β domain of PfEMP1, the crystal structure can be used as template to model and further elucidate possible ICAM-1 binding residues in the DBL2β domain (Tolia et al., 2005).

Another DBL crystal structure has recently been constructed, the *P. knowlesi* DBL domain (Pkα-DBL) to 3Å (Singh et al., 2006). Like EBA-175 Pkα-DBL is an erythrocyte invasion protein, and has a sequence that 71% homologous with the EBA-175 F1 and F2 sequences. However, Pkα-DBL interacts with Duffy antigen receptor chemokines (DARC) rather than GpA.

The implications of these two crystallized DBL structures on *Plasmodium falciparum* erythrocyte adhesion and immune invasion have been considered by Howell et al. (2006). The crystal structures of EBA-175 and Pkα-DBL can be

used to make inferences about other EBL members especially their binding pockets. Only variant antigens belonging to two species of *Plasmodium* contain DBL domains. Due to their common sequences and encoded domains, it has been suggested that *Plasmodium falciparum var* genes may have evolved from *ebl* genes. Further evidence that EBL binding pockets may be similar is that all studied EBL family members bind at least one sialoglycoprotein (ie. DARC, GpA).

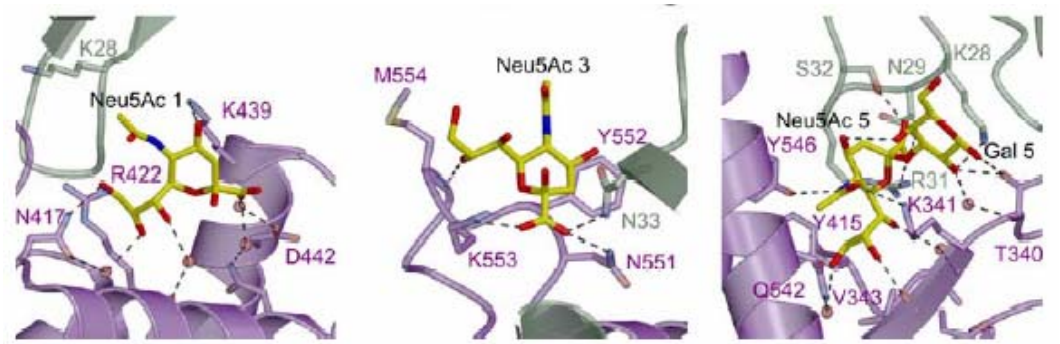

Figure 8- View of three of the glycan binding sites of EBA-175, glycan 1, 3 and 5 are shown from left to right (Tolia et al., 2005).

Difficulties of a Malaria Vaccine

In general, there are two ways to induce immunity: non-natural immunity and natural immunity. Natural immunity occurs after exposure to disease, while non-natural immunity is achieved by triggering immune mechanisms against the disease through the use of a vaccine (Good, 2001). In the case of malaria, natural immunity takes years of exposure in an endemic area to develop. The natural immunity acquired to the *Plasmodium* parasite is usually not sterile immunity but clinical immunity where the individual does not show the clinical symptoms associated with malaria but still carries a low level of parasites in their blood (Good, 2001). In sterile immunity the body is completely rid of all *Plasmodium* parasites. Individuals with clinical immunity can still continue the *Plasmodium* lifecycle through the transmission of *Plasmodium* gametocytes. If a vaccine was designed that conferred sterile immunity, eradication of certain species of *Plasmodium* may be possible. However, even a vaccine that provided clinical immunity would be a great move forward in the destruction of this disease.

Plasmodium is antigenically different from stage to stage of its lifecycle, and different immune responses are required for each stage (Good, 2001). Vaccine development is much further along in the mosquito stage than in the blood stage. However, it is the blood stage that is responsible for disease. There are many factors that are impeding the development of a vaccine for this stage including the complex lifecycle of *Plasmodium*, the use of antigenic variation, and the

immunological non-responsiveness of some individuals to the proteins that comprise the vaccine (Good, 2001).

Many successful vaccines for other diseases such as polio and smallpox were simple vaccines that were composed of killed or attenuated organisms (Good, 2001). These vaccines display the entire antigenic selection. In malaria this method is not very applicable. *Plasmodium* replicate within IE's during the blood stage of the lifecycle and place their antigenic proteins on the surface of the IE's (Miller et al., 2002). Therefore, using a killed or altered form is not possible.

Another possible vaccine type is a subunit vaccine. A subunit vaccine is a vaccine that is composed of some of the antigens of the organism but not the entire antigenic component. However, this vaccine is problematic due to the fact that *Plasmodium* parasites have the ability to change their antigenic components over the course of an infection. Another problem arises from the fact that there is considerable allelic variation between strains (Good, 2001). There are also inherent problems in forming a subunit vaccine such as ensuring the proper folding of proteins to maintain their antigenic properties. It is unlikely that a single antigen subunit vaccine will be able to protect against the various *Plasmodium falciparum* strains. In order for a vaccine to be effective, the method of exposure of the antigens to the immune system will probably need to be very different from the method used by *Plasmodium* during a normal course of infection (Good et al., 2004).

There are many factors that need to be taken into consideration when forming a malaria vaccine. Besides the scientific challenges of designing a vaccine there are also many geographic and economic factors to be considered. However, the need for a malaria vaccine is high as strains of malaria continue to become drug resistant (Good, 2001).

Purpose

The purpose of this project is to identify amino acid residues involved in binding of the variant antigen protein PfEMP1 to ICAM-1. ICAM-1 is believed to be responsible for the sequestering of *P. falciparum* infected erythrocytes in the brain. This sequestration is associated with the disease cerebral malaria (Miller et al., 2002). In order to determine some of the amino acid residues of this domain that are responsible for ICAM-1 binding, I performed an alanine substitution of certain residues that I predicted to be involved with binding.

Previous experiments describing the regions of DBL2β involved in the adherence of ICAM-1 were done by deleting large segments of the protein. However, in this experiment none of the amino acid residues were deleted, instead a single residue was changed to an alanine. The main advantage to this method is that the structure of the protein will not be severely altered. Therefore, any changes in binding will most likely be due to altering an amino acid involved in binding rather than altering the structure to the extent that the protein will no longer bind (Clackson et al., 1995).

The most important reason for determining the residues of PfEMP1 involved in adherence to ICAM-1 is that PfEMP1 are likely targets for a vaccine against cerebral malaria. DBLβ domains are unique to *P. falciparum* and PfEMP1 is known to be a target of antibodies in people who have developed immunity.

Since the domains involved in ICAM-1 binding are highly conserved among different strains of *Plasmodium*; it might provide a strain transcendent vaccine. Also, sequestering of IE's during the blood stage of the *Plasmodium falciparum* life cycle is believed to contribute to pathogenesis. Understanding the residues and mechanisms involved in ICAM-1 binding could aid in the development of drugs that prevent the binding of IE's to ICAM-1 which could not only decrease the severity of the symptoms of malaria but might also promote or increase destruction of IE's by the spleen. In general the purpose of this experiment is to further the knowledge of malaria disease, which in time may lead to the development of a drug or vaccine to treat this illness.

MATERIALS AND METHODS

Part 1: Analysis of DBL2βc2 Binding Region

The amino acid sequence of the DBL2βc2 region of A4tres (gene identification # AF193424) was sent to ExPASy Proteomics Server of the Swiss Institute for Bioinformatics. The SWISS-MODEL program performs comparative modeling. This program was used to form a plausible three dimensional structure of the A4tres sequence. The A4tres structure was based on the crystal structure of EBA-175. I supplied the Pdb reference for EBA-175, and chose this structure because it also contains a DBL2β region. The Deep View Swiss-Pdb Viewer was then used to manipulate the structure, and based on this structure I chose 3 amino acid residues to exchange with alanine.

Part 2: Primer Construction and Mutagenesis

The primers were based on the beginning of the A4tres DBL2βc2 template. The expression vector for the DBL2βc2 domains was T8-12CA5 designed by Erik Whitehorn of Affymax,Inc. (Santa Clara, CA). I viewed the sequences using the program Artemis (Rutherford et al., 2000), and designed the primers according to the parameters set by the QuikChange Site-Directed Mutagenesis Kit (Stratagene, La Jolla CA). They ranged from 32-36 nucleotide bases in length

and contained the desired mutation towards the center of the primer. The primer sequences (table 1) were ordered from IDT (Integrated DNA Technologies, Coralville IA).

Table 1: Table of primers ordered from IDT containing modifications for the associated substituted amino acid

Amino Acid to be Mutated:	Primers
Lysine (K) to Alanine (A)	5'GCAAAACAGAAGAGGTTGGCGACTGGTACCCCAAGG'3 5'CCTTGGGGTACCAGTCGCCAACCTCTTCTGTTTTGC'3
Glutamate (E) to Alanine (A)	5'GCAAAACAGACGAGGTTGGAAACTGGTACCCC'3 5'GGGGTACCAGTTTCCAACCTCGTCTGTTTTGC'3
Threonine (T) to Alanine (A)	5'CTGCAGTGACATACAGCGAAACAGAAGAGGTTGG'3 5'CCAACCTCTTCTGTTTCGCTGTATGTCACTGCAG'3

The mutagenesis reaction was performed using the QuikChange Site-Directed Mutagenesis Kit according to the manufacture's instructions. The kit also required a thermal cycler (FTGENEJD, Techne, Minneapolis MN) and 50 ng of the A4tres DBL2βc2 plasmid DNA (Smith et al., 2000) per mutagenesis. The reaction was prepared with 5 μL x 10x reaction buffer, 125 ng of each oligonucleotide primer, 1 μL of dNTP mix, and brought up to a final volume of 50 μL. 1 μL of *PfuTurbo* DNA polymerase was added to mixture just before the reaction was placed in a thermal cycler with a hot top assembly.

The mutagenesis reactions were run using the following parameters for the mutant containing an alanine substitution for lysine:

1 cycle at 95°C for 30 seconds

16 cycles at 95°C for 30 seconds

16 cycles at 55°C for 1 minute

16 cycles at 68°C for 9 minutes

The reactions to generate alanine substitutions for glutamate and threonine were run using similar parameters except that instead of the reaction being run for 16 cycles it was run for 12 cycles. The number of cycles was decreased because these reactions generated a single base change. In the mutant containing an alanine substitution for lysine two bases were changed.

The amplification was then confirmed by running 10 μL of the reaction products on a 1% agarose gel. 1 μL of *Dpn* 1 was added to the reaction mixture in order to digest non-mutated parental DNA template. The digest was incubated for 1 hour at 37°C.

Part 3: Transformation of Mutagenized DNA

Once the digestion was complete, 1 μL of *Dpn* 1-treated DNA was added to 50 μL of XL1-Blue supercompetent cells (Stratagene, La Jolla CA). The reaction was incubated on ice for 30 minutes. Then the mixture was heated for 45 seconds at 42°C and placed on ice for 2 minutes to facilitate the uptake of the plasmid

DNA into the bacteria. 500 µL of Luria-Bertani broth (LB) was added to the transformation, and it was incubated at 37°C for an hour while shaking. Then 250 µL of the mixture was plated on Amp plates and allowed to grow overnight. The plates were stored at 4°C.

Part 4: Plasmid DNA Isolation

Overnight cultures were made of the transformed *E. coli* cells and the plasmid DNA was isolated using the QIAprep Spin Miniprep Kit (Qiagen Corp, Valencia CA). The overnight cultures were prepared by inoculating 4 mL LB broth, 40 µL ampicillin, with 1 colony of transformed *E. coli* cells. This culture was then incubated at 37°C overnight while shaking. The cultures was then transferred to a microcentrifuge tube and centrifuged for 45 seconds. The supernatant was removed and the pellet was used in the plasmid DNA isolation.

For DNA isolation the pellet was resuspended in 250 µL P1 buffer which contains RNase A. 250 µL of P2 buffer was added to the mixture and the microcentrifuge tube was inverted 6 times to ensure proper mixing. The P2 buffer lyses the bacteria and contains NaOH / SDS. 350 µL of N3 buffer was then added to the microcentrifuge tube and again inverted 6 times. The N3 buffer is a neutralization buffer that produces high-salt conditions. These conditions cause the denatured proteins, chromosomal DNA, cell debris, and SDS to precipitate out of solution. The microcentrifuge tube was then centrifuged for 10 minutes at

10,000 rpm. The supernatant was then added to a spin column and centrifuged for 1 minute. The flow through was discarded. The plasmid DNA was washed with 750 μL PE buffer. The flow through was removed. The spin column was centrifuged for an additional minute to ensure the entire buffer had been removed. 50 μL of EB buffer was added to the spin column to elute the plasmid DNA, and centrifuge for 1 minute. The plasmid DNA was then stored at 4°C. Plasmid DNA was isolated using this method for both the non-mutated A4tres DBL2βc2 and FCR3 DBL2βc2 plasmid DNA as well as the alanine substituted A4tres DBL2βc2 mutants. DNA of each mutant was sent to Elim BioPharamceuticals, Inc (Hayward, CA) for sequencing.

Part 5: Plasmid DNA Transfection

The plasmid DNA was transfected into COS-7 cells which were kindly provided by D. Howell (SBRI, Seattle WA). The COS-7 cells were grown in DMEM+ medium (containing FBS, L-glutamine, Hepes, and Penicillin / Streptomycin), mediated in a 37°C CO_2 incubator, and maintained according to standard cell culturing techniques. The transfections were performed under sterile conditions. To prepare for the transfections, COS-7 cells were first seeded to coverslips. 4 coverslips were placed in each 35mM well and covered with approximately 1 x10^5 cells in 2 mL of medium. The coverslips were pressed and forced to adhere by surface tension to the bottom of the wells. Then the cells

were incubated at 37°C in a CO_2 incubator until they were 30-50% confluent (next day).

To transfect the cells, 1 μg of appropriate plasmid DNA was diluted with 125 μL of Opti-MEM (Invitrogen, Carlsbad CA). The plasmid DNA dilutions were repeated for each well. Then, in a separate microcentrifuge tube, 12 μL x number of wells of Optifect reagent (Invitrogen, Carlsbad CA) was mixed with 125 μL x number of wells of Opti-MEM, and allowed to incubate for 5 minutes. After the 5 minute incubation, the diluted plasmid DNA was combined with 137 μL of the Opti-MEM / Optifect reagent mixture, and allowed to incubate at room temperature for at least 20 minutes. After the incubation, the entire volume of each plasmid DNA mixture was added to the appropriate well. The transfection mixture was equally distributed over the cells by rocking the 6-well plate. The cells were then incubated at 37°C in a CO_2 incubator for 48 hours.

Part 6: ICAM-1 Coating of Dynabeads

Before the binding assay could be performed on the transfected COS-7 cells, the magnetic Dynabeads (Invitrogen, # 112.01D) needed to be coated with ICAM-1. The M280 Dynabeads (700,000 beads / μL) are covered with a sheep anti-mouse IgG. The ICAM-1 used to coat the Dynabeads is a human ICAM-1/Fc recombinant fusion protein (R & D systems, 720-1C). In order for the human IgG1 Fc fragment to attach to the anti-mouse IgG on the bead an intermediate

antibody was used. This antibody is an Affinipure Mouse anti-human IgG Fc gamma fragment (Jackson, #209 005 098), with a concentration of 1.8 μg / μL.

The beads were first washed in washing and coating buffer (1 X PBS (pH 7.4), 0.1% BSA). For 12 coverslips, 60 μL of the bead solution was transferred to a microcentrifuge tube. The tube was then placed in a Dynal Particle Concentrator (Dynal, Oslo) and the supernatant was pipetted off. The beads were resuspened in 700 μL of washing and coating buffer. The wash was repeated once more.

To coat the beads with Anti-human-Fc antibody, the beads were resuspended in washing and coating buffer containing 2 μg of Anti-human-Fc antibody. The beads were then incubated for 3 hours at room temperature or overnight at 4°C. The unbound antibody was washed off. Again the microcentrifuge tube was placed in a Dynal magnet and the supernatant was pipetted off. The beads were resuspended in 700 μL of washing and coating buffer. The wash was repeated twice more.

The bead suspension was split into two equal volumes. One of the volumes was resuspened in 150 μL of washing and coating buffer containing 6 μg of ICAM-1/Fc. The other volume was used as a control and was resuspened in 150 μL of just washing and coating buffer. The two volumes were then incubated for 3 hours at room temperature or overnight at 4°C.

Part 7: Binding Assay

To prepare for the binding assay, binding medium was made by mixing 1 X RPMI (25mM HEPES, glutamine and glucose, without bicarbonate) and BSA to 0.5%. The mixture was heated to 37°C and then the pH was adjusted between 7.1 - 7.3. The unbound ICAM/Fc was washed off the beads by resuspending them in 700 μL of binding medium. The wash was repeated on both of the volumes of beads twice more, and then the beads were resuspended in binding medium to a volume of 25 μL/coverslip.

By now the seeded coverslips had been incubating at 37°C in the CO2 incubator for 48 hours. To begin the binding assay, the coverslips containing the transfected COS-7 cells were transferred to new 6-well plates. One coverslip was placed cell side up in each well, and the bottom of the coverslip was wicked dry before it was transferred. Subsequently 25 μL of bead suspension was placed on each coverslip. Since there are 4 identical coverslips for each mutant and control, 2 of each type of coverslip was covered with ICAM-1 bound beads, while the other two were used as controls and covered with beads that were not coated with ICAM-1. The 6-well plates containing the coverslips were placed in a humidified chamber (covered Tupperware dish lined with wet paper towels), and incubated in a warm room at 37°C for 45 minutes.

After the incubation, a coverslip stand (Pasteur pipette tips bent at a right angle) was placed in each well of plates containing a coverslip. 8 mL of binding

medium was added to each well very slowly to avoid agitating the beads. Each coverslip was flipped (cell side down) carefully, attempting to keep the entire coverslip in the medium, onto a stand to permit the unbound beads to fall off. The unattached beads were allowed to decant for 10 minutes at room temperature. Afterward, the coverslips (cell-side up) were transferred to new 6-well plates containing 2% paraformaldehyde, and fixed for 20 minutes.

Part 8: Immunofluorescence Assay

PfEMP1 domains are expressed transiently in COS-7 cells. Therefore, one needed a way of differentiating the cells that were expressing the PfEMP1 proteins from those that were not. The construct used contained an HA peptide tag, which would be expressed on the surface of cells that were expressing PfEMP1. The immunofluorescence assay uses an Alexa488-conjugated anti-HA antibody (Invitrogen, Zymed) to bind to the HA on the surface of the cell. Consequently, cells expressing the PfEMP1 protein will appear green under a fluorescence microscope. All of the cell nuclei are also stained with DAPI (4, 6-diamadino-2-phenylindole) to ease the determination of cell number.

To perform the immunofluorescence assay, initially the coverslips were washed (1 X PBS) 3 consecutive times to remove the paraformaldehyde. On a sheet of parafilm, the locations of the coverslips to be assayed were marked. Then a humidified chamber (see binding assay) was prepared, and the parafilm

sheet was placed inside. On each of the marked locations, 25 μL of Alexa488-HA antibody (diluted 1/250 from stock) was placed. The appropriate coverslip was carefully placed cell-side down on each of the droplets of antibody ensuring that the surface of the coverslip was completely covered. Also, before the coverslip was positioned on the droplet of antibody, the coverslip was wicked dry. The humidified chamber was then covered and the cells incubated for 45minutes to an hour.

After the incubation, the coverslips were briefly washed. Each coverslip was wicked dry on a Kimwipe (Fisher Scientific International Inc., Hampton NH), dipped 5 times in washing and coating buffer, and then wicked dry again. After washing, the coverslips were placed directly in 1 X PBS (cell-side up), and allowed to soak for at least 10 minutes (sometimes overnight).

Ultimately, the coverslips were mounted on slides. Since 4 coverslips were mounted on each slide, 4 droplets of DAPI (approximately 4 μL) were arranged on each slide. The coverslips were placed cell-side down on the droplets of DAPI, and the edges sealed using nail polish (L'Oreal). The mounts were allowed to set for at least 30 minutes at 4°C, and were otherwise stored in a slide box at 4°C.

Part 9: Quantifying Cells

The cells were qualified and quantified based on brightness, color, and number of bound beads. When viewing the cells, the overall brightness of the Alexa488 dye was noted (example: bright, medium, dull). For each construct at least 50 cells expressing PfEMP1 were counted. When counting the cells in the field of the microscope, the number of green cells vs. the number of DAPI stained cells are recorded. The number of green cells vs. the number of green cells with beads was also recorded. Lastly the number of beads per cell was estimated/counted, and a rough average was obtained for the construct. The standard deviation of the average number of beads per cell for each clone was also calculated using Excel.

RESULTS

In order to make a more educated guess as to what amino acid residues would be involved in ICAM-1 binding I sent the amino acid sequence of the DBL2βc2 region of A4tres to ExPASy Proteomics Server of the Swiss Institute for Bioinformatics. This program performed comparative modeling, and produced a three dimensional structure of the A4tres sequence (Figure 9). Using the Deep View Swiss-Pdb Viewer to manipulate the structure, I chose 3 amino acid residues to change to alanine: a lysine residue at position aa831, a glutamate residue at position aa834, and a threonine residue at position aa837 (Figure 10).

After I had chosen the amino acids to be converted to alanine, I designed primers to be used in the mutagenesis reactions (Table 1). The PCR products for those reactions were initially checked by electrophoresis to ensure that they were of the proper size (Figure 11). Once the mutant plasmids were isolated, I sent 1.5 μg of each plasmid along with T8uni5A primer for DNA sequencing. Upon the return of those sequences, I compared them to the original A4tres sequence and found that the mutagenesis reactions had been successful.

The binding/immunofluorescence assays were performed to examine the A4tres mutants' ability to bind ICAM-1. In the binding assay, the cells were incubated with beads coated with ICAM-1, while in the immunofluorescence assay the same cells were incubated with Alexa488-conjugated anti-HA antibody, DAPI. DAPI stains the nuclei of the cells blue and the Alexa488 labeled antibody

made the cells expressing PfEMP1 appear green. After the binding/ immunofluorescence assays were completed, the transfected COS-7 cells were mounted on slides and viewed using fluorescence microscopy. At least 50 cells showing surface expression of the construct from 2 different clones of each mutant were qualified and quantified based on brightness and number of bound beads. Whenever possible, counting cells on the outer edges of the coverslips was avoided due to the fact that the beads did not always evenly distribute around the coverslip. Table 2 summarizes the results obtained for the 3 mutants. In general, the green fluorescence (Alexa488) displayed by the mutants was bright indicating that the construct was being highly expressed. Also, all of the mutants bound ICAM-1 covered beads to varying degrees.

Table 2 – Summary of results obtained from binding/ immunofluorescence assays. The "Percent Binding ICAM-1" column shows the percent of cells expressing the construct that bound ICAM-1.

	Percent Binding ICAM-1	Average # of Beads / Cell	Standard Deviation of Average	Fluorescence Intensity	Transfection Percentage
Lysine-Alanine Clone 1	100 ± 0	68.1	40.3	Bright	51.0
Lysine-Alanine Clone 2	100 ± 0	64.5	37.8	Bright	71.6
Glutamate-Alanine Clone 1	100 ± 0	93.9	37.5	Bright	82.5
Glutamate-Alanine Clone 2	100 ± 0	96.8	86.1	Bright	48.2
Threonine-Alanine Clone 1	98.2 ± 1.7	33.9	20.7	Bright	87.7
Threonine-Alanine Clone 2	96.3 ± 3.7	50.3	28.8	Bright	59.3
A4tres-Clone 1 (+ control)	100 ± 0	77.1	41.4	Bright	45.5
A4tres-Clone 2 (+ control)	100 ± 0	68.1	37.5	Bright	45.5
FCRvarCSA-Clone 1 (- control)	0 ± 0	0	0	Bright	51.4
FCRvarCSA-Clone 2 (- control)	0 ± 0	0	0	Bright	39.7

A4tres and FCRvarCSA were the positive and negative controls respectively (figures 12, 13, 17). As expected, the green cells expressing FCRvarCSA did not bind any beads since FCRvarCSA does not bind ICAM-1. All cells expressing A4tres however bound ICAM-1 covered beads. The average number of beads per cell was 77.1 and 68.1 for clones 1 and 2 respectively. For all 102 green cells counted, the average number of beads per cell was 72.6. The transfection efficiency for A4tres was 45.5% while the transfection efficiencies for FCRvarCSA ranged from 39.7 – 51.4%, and averaged 45.6%.

In the clones where lysine (aa831) was converted to alanine (figures 15, 19), all of the cells expressing the modified DBL2β2c2 domain (green cells) bound ICAM-1. On average the number of beads per cell was less for the lysine mutant than for the A4tres control. For clone 1 there was an average of 68.1 beads per cell, while the average number of beads per cell for clone 2 was 64.5. Beads were counted on a total of 104 green cells with the overall average being 66.3 beads per cell. The transfection efficiencies ranged from 50.0-71.6%, and averaged 59.8%.

In the clones where glutamate (aa834) was converted to alanine (figures 14, 18), all of the green cells also bound ICAM-1. The average number of beads per cell for clone 1 was 93.9 while the average number of beads per cell for clone 2 was 96.8. Beads were counted on a total of 107 green cells with the overall average being 95.4 beads per cell. The transfection efficiencies ranged from 82.5-48.2%, and averaged 65.4%.

When threonine (aa837) was converted to alanine (figures 16, 20) almost all of the green cells bound ICAM-1 coated beads. There were 3 green cells that did not contain at least 5 beads. The average number of beads per cell for clone 1 was 33.9 while the average number of beads per cell for clone 2 was 50.3. Beads were counted on a total of 108 green cells with the overall average being 42.1 beads per cell. The transfection efficiencies ranged from 59.3-87.7 %, and averaged 73.5%.

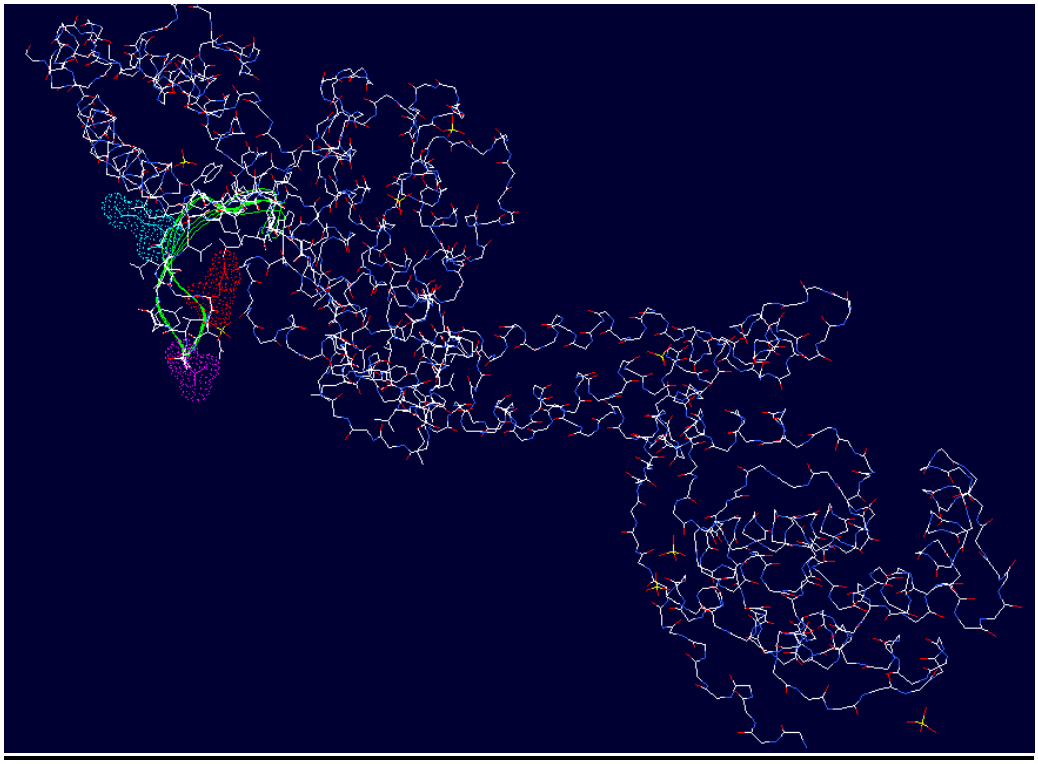

Figure 9- Overall picture of the DBL2β region of A4tres. This image was generated by the ExPASy Proteomics Server of the Swiss Institute for Bioinformatics from the crystal structure of EBA-175 (Guex et al., 1997). The green ribbon runs along the amino acids that were shown to be important for binding ICAM-1 in the deletion experiments performed by Springer et al. (2004).

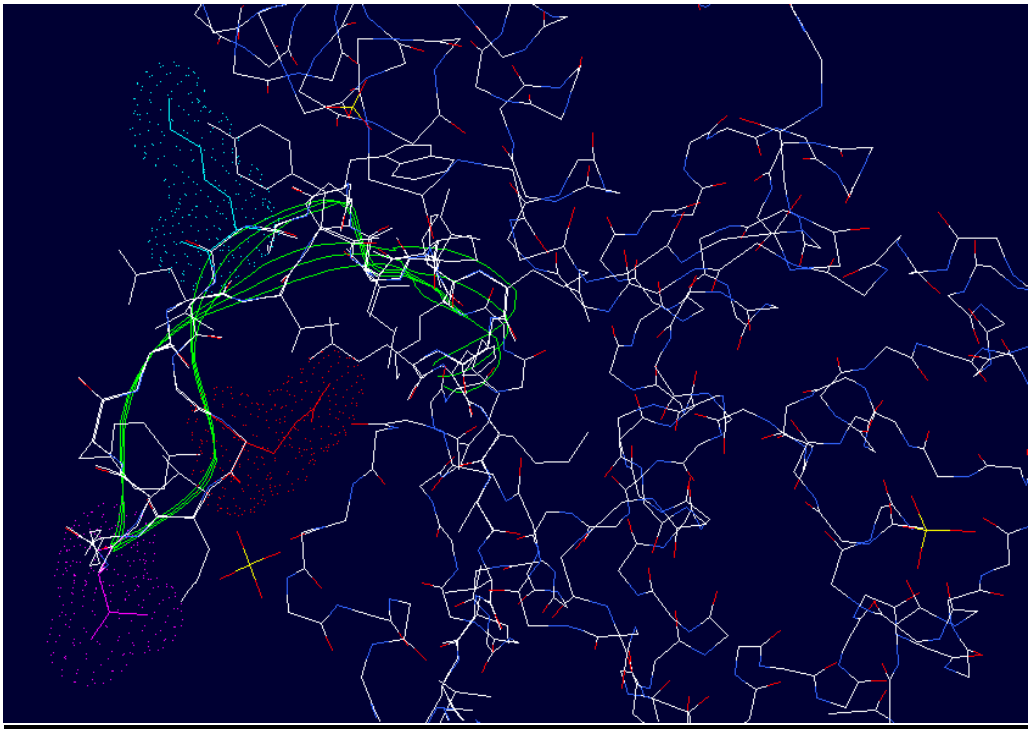

Figure 10- Close up of the possible ICAM-1 binding region, and the three amino acids chosen to be substituted with alanine (Guex et al., 1997). The R-group highlighted in light blue is from lysine, the R-group in red in from glutamate and the R-group in purple is from threonine.

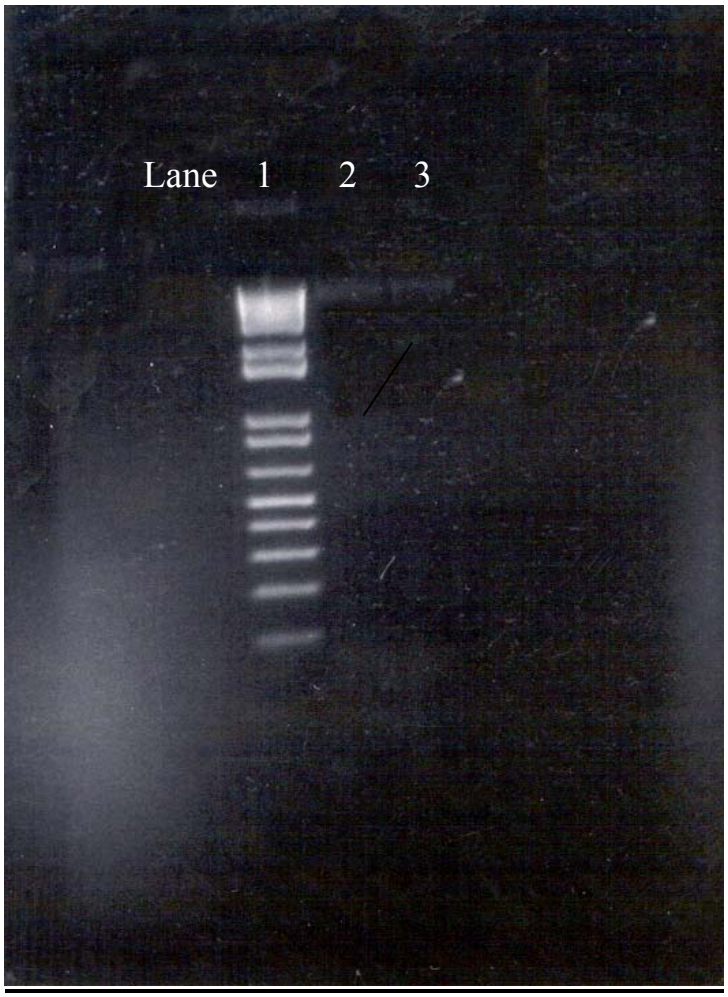

Figure 11- 10 μL of site-specific mutagenesis PCR products from 2 mutagenesis reactions were run on a 1% agarose gel. The 1 Kb ladder is in lane 1, lane 2 contains the products of the reaction where glutamate was converted to alanine, and lane 3 contains the products of the reaction where glutamate was converted to alanine. The products seemed to have the correct molecular weight of approximately 9500 bp.

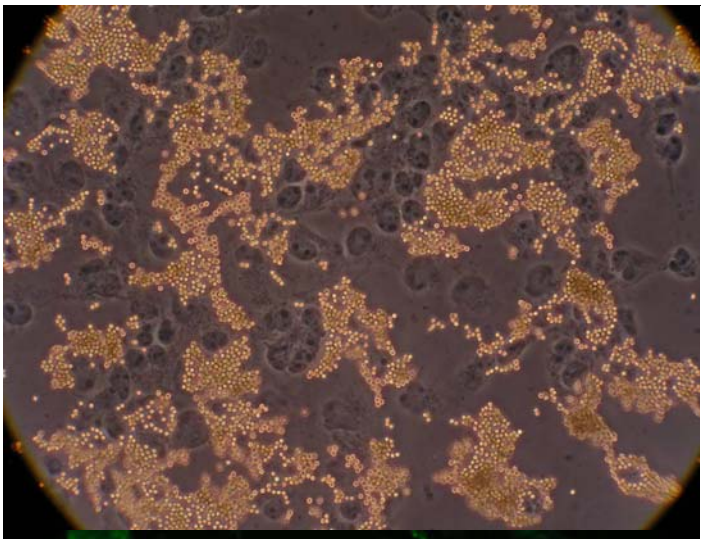

Figure 12a- **A4tres** (+ control) transfected COS-7 cells binding ICAM-1 covered beads. This is a view of a high density cluster of cells that was not used for counting due to the difficulty in discerning which cells were binding beads.

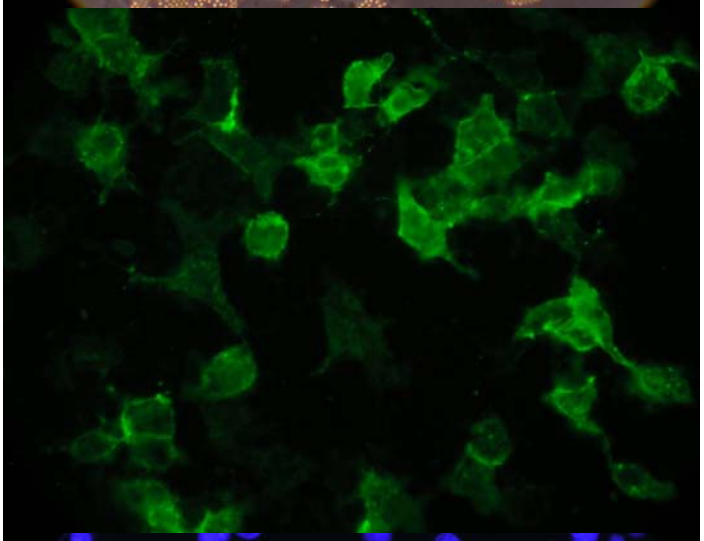

Figure 12b- Fluorescent image of the same A4tres transfected COS-7 cells seen in figure 12a. All of the green cells are expressing A4tres. Notice that the green cells are the same cells binding beads in figure 12a.

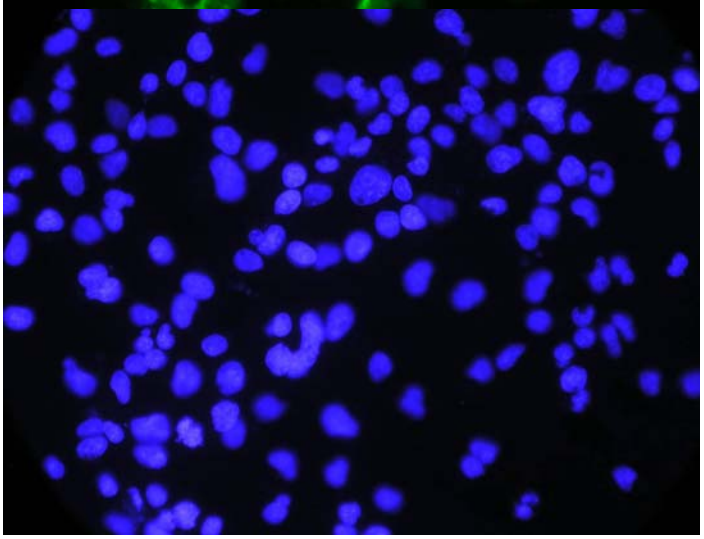

Figure 12c- Fluorescent image of the DAPI stained nuclei of the cells seen in figures 12a and 12b. Obviously a large portion of the cells are not expressing the A4tres construct.

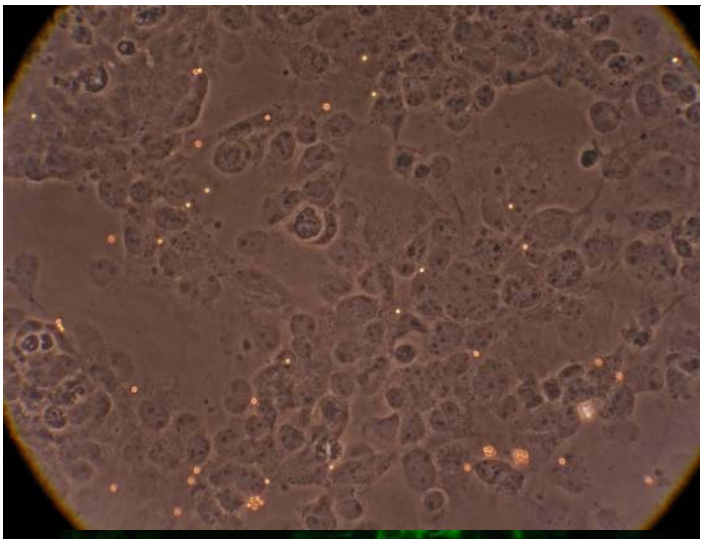

Figure 13a- **FCRvarCSA** (- control) transfected COS-7 cells binding ICAM-1 covered beads. This is a view of a high density cluster of cells.

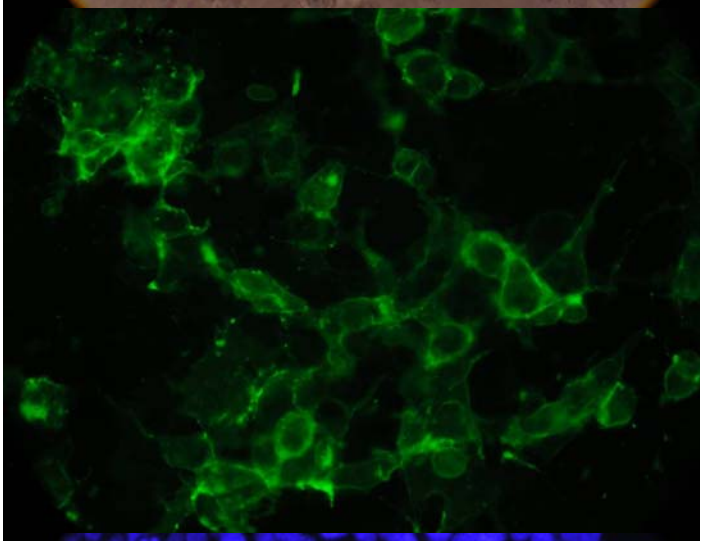

Figure 13b- Fluorescent image of the same FCRvarCSA transfected COS-7 cells seen in figure 13a. All of the green cells are expressing FCRvarCSA. Notice that the green cells are not binding beads.

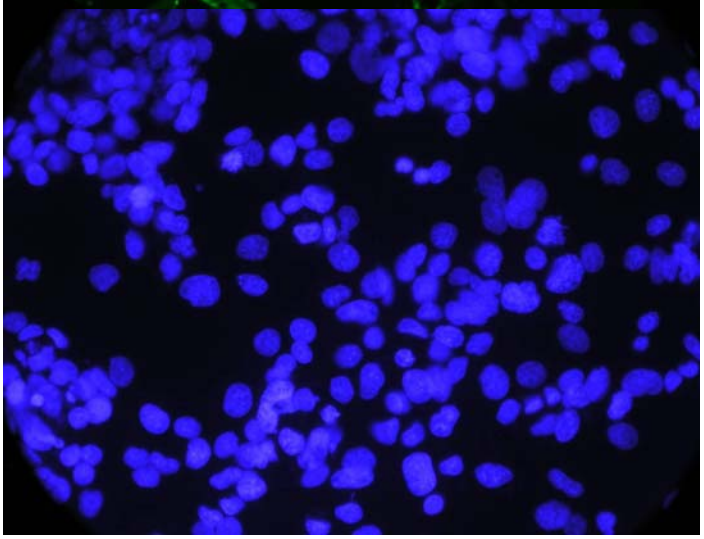

Figure 12c- Fluorescent image of the DAPI stained nuclei of the cells seen in figures 13a and 13b. Obviously a large portion of the cells are not expressing the FCRvarCSA construct.

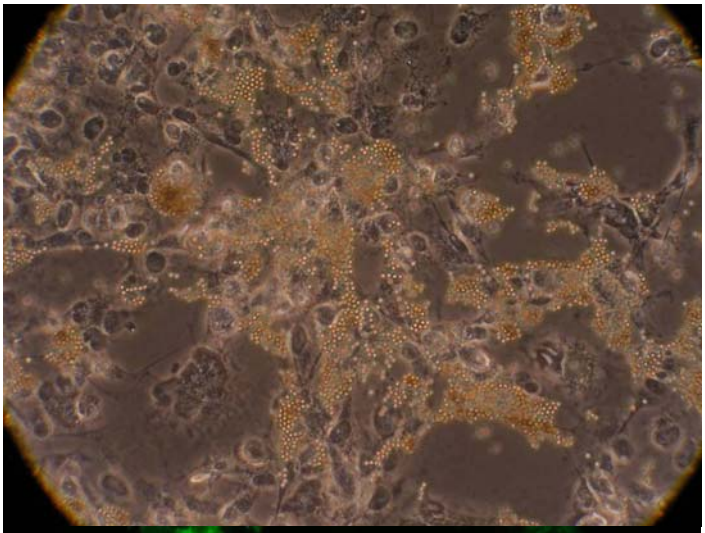

Figure 14a- COS-7cells transfected with the **glutamate to alanine** mutant binding ICAM-1 covered beads. This is a view of a high density cluster of cells that was not used for counting due to the difficulty in discerning which cells were binding beads.

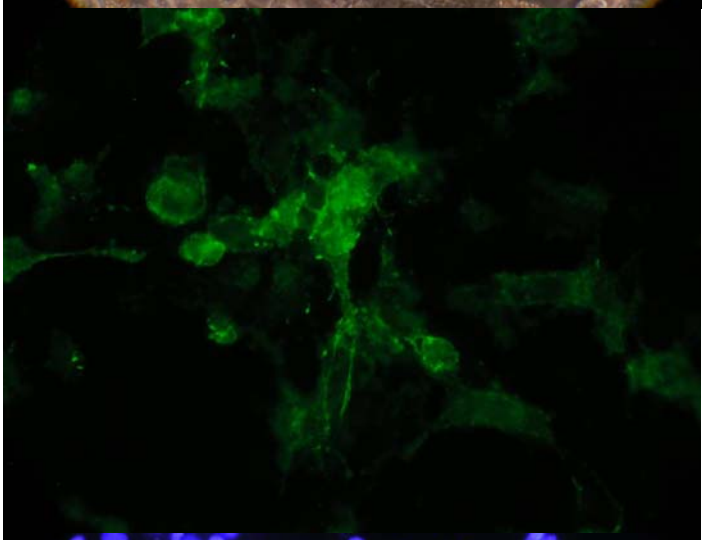

Figure 14b- Fluorescent image of the same transfected COS-7 cells seen in figure 14a. All of the green cells are expressing the construct. Notice that the green cells are the same cells binding beads in figure 14a.

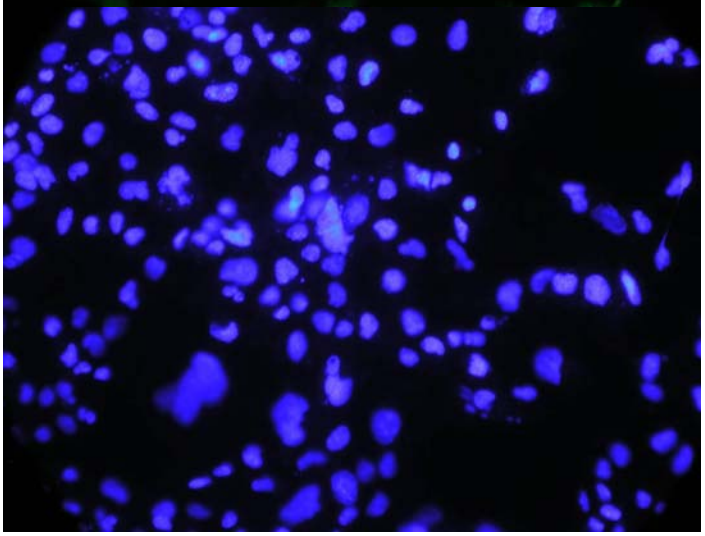

Figure 14c- Fluorescent image of the DAPI stained nuclei of the cells seen in figures 14a and 14b. Clearly a large portion of the cells are not expressing the glutamate to alanine construct.

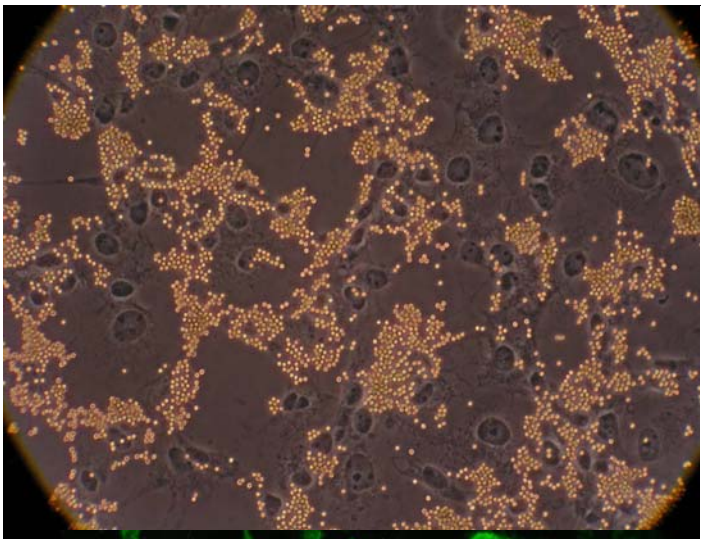

Figure 15a- COS-7cells transfected with the **lysine to alanine** mutant binding ICAM-1 covered beads. This is a view of a high density cluster of cells that was not used for counting due to the difficulty in discerning which cells were binding beads.

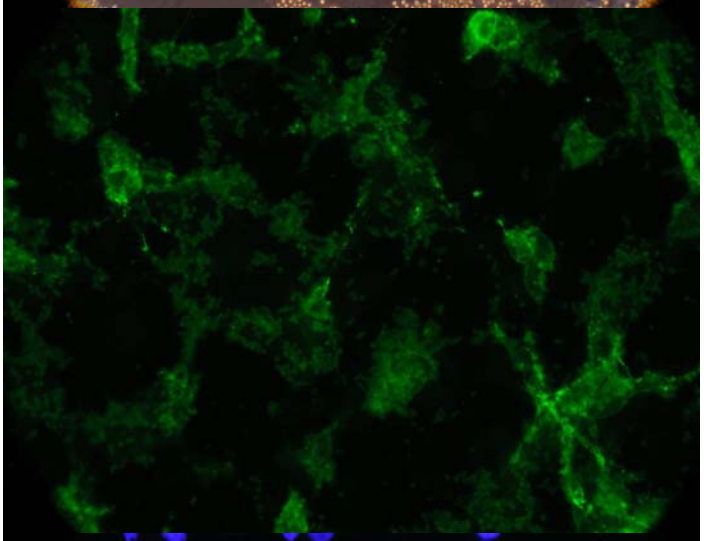

Figure 15b- Fluorescent image of the same transfected COS-7 cells seen in figure 15a. All of the green cells are expressing the construct. Notice that the green cells are the same cells binding beads in figure 14a.

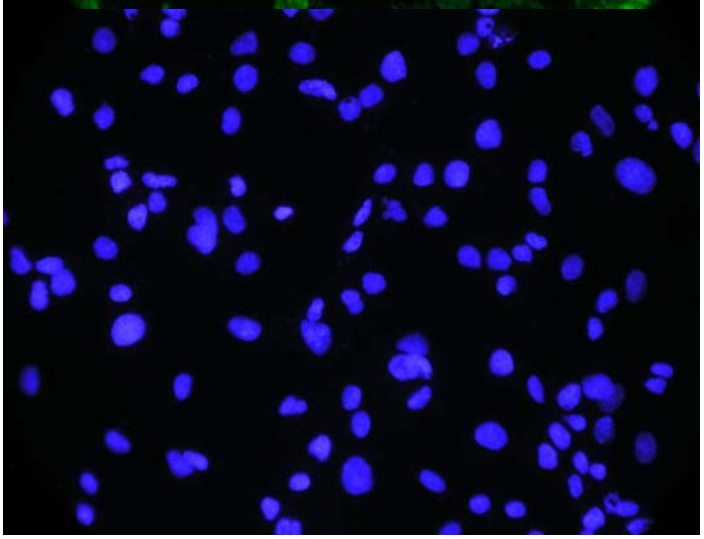

Figure 15c- Fluorescent image of the DAPI stained nuclei of the cells seen in figures 15a and 15b. Clearly a large portion of the cells are not expressing the lysine to alanine construct.

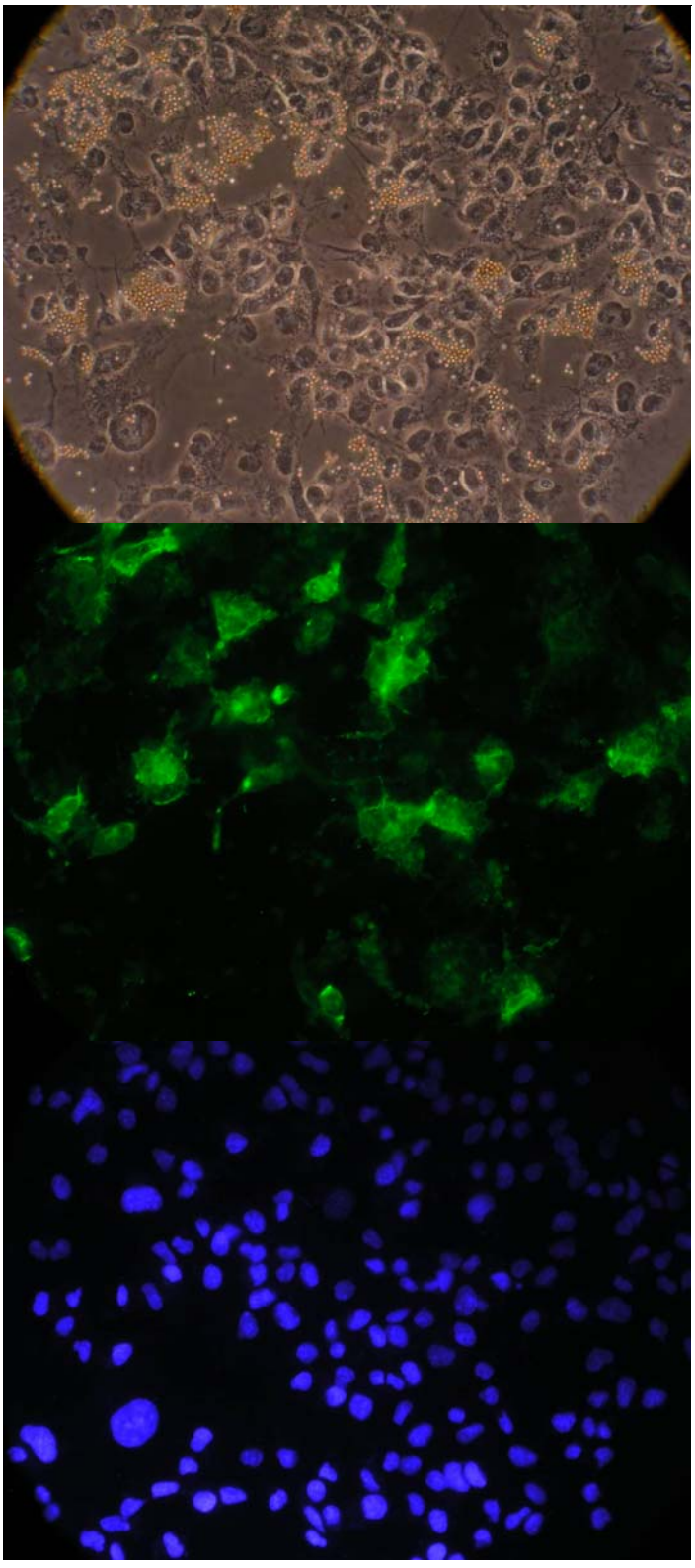

Figure 16a- COS-7cells transfected with the **threonine to alanine** mutant binding ICAM-1 covered beads. This is a view of a high density cluster of cells that was not used for counting due to the difficulty in discerning which cells were binding beads. However, notice the lack of beads as compared to figures 12, 14, and 15.

Figure 16b- Fluorescent image of the same transfected COS-7 cells seen in figure 16a. All of the green cells are expressing the construct. Most of the green cells are binding beads, but there some that appear to be binding less than 5 beads.

Figure 16c- Fluorescent image of the DAPI stained nuclei of the cells seen in figures 16a and 16b. Clearly a large portion of the cells are not expressing the threonine to alanine construct.

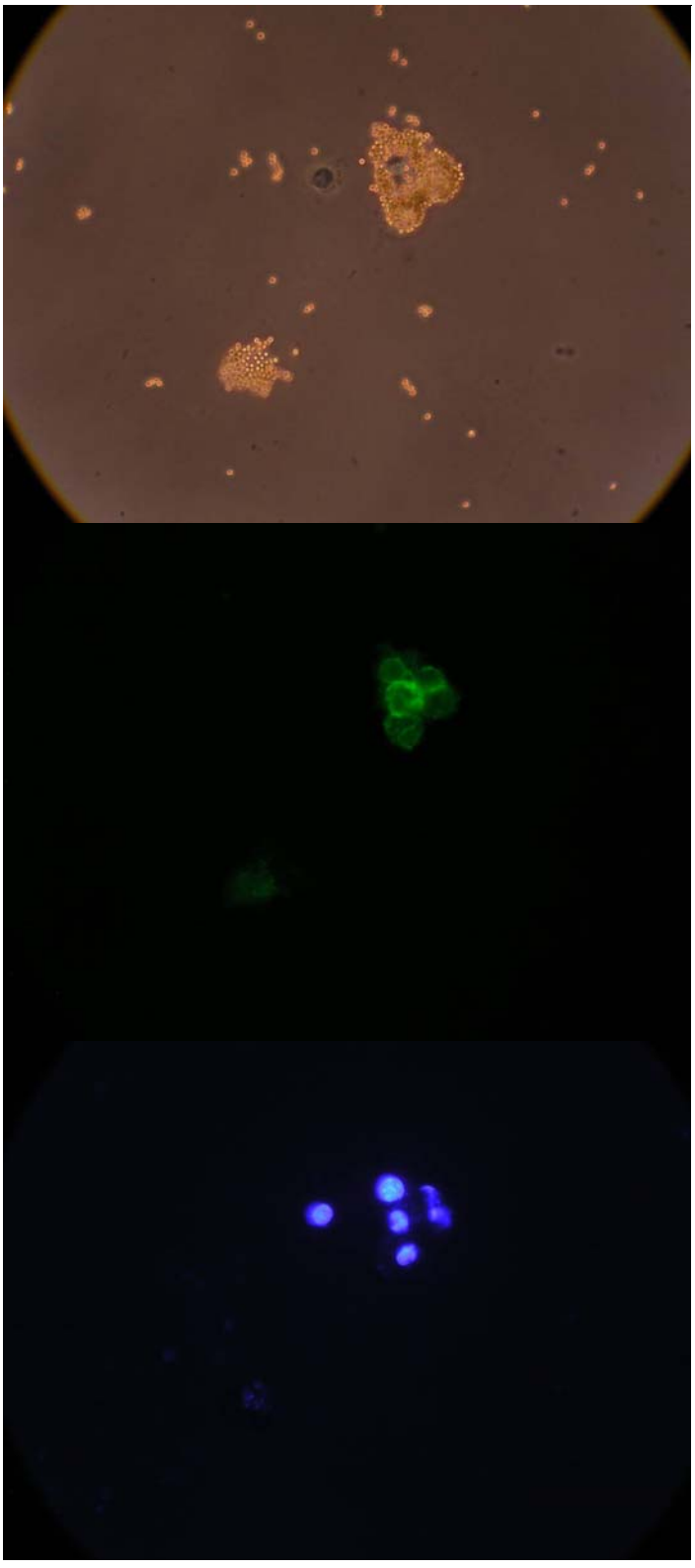

Figure 17a- COS-7cells transfected with **A4tres** binding ICAM-1 covered beads. This is a representative example of the type of view used for counting, and the amount of beads bound by A4tres.

Figure 17b- Fluorescent image of the same transfected COS-7 cells seen in figure 17a. All of the green cells are expressing the construct, and binding ICAM-1 covered beads.

Figure 17c- Fluorescent image of the DAPI stained nuclei of the cells seen in figures 17a and 17b. Notice how this example skews the transfection efficiency as compared to the less constricted view in figure 12.

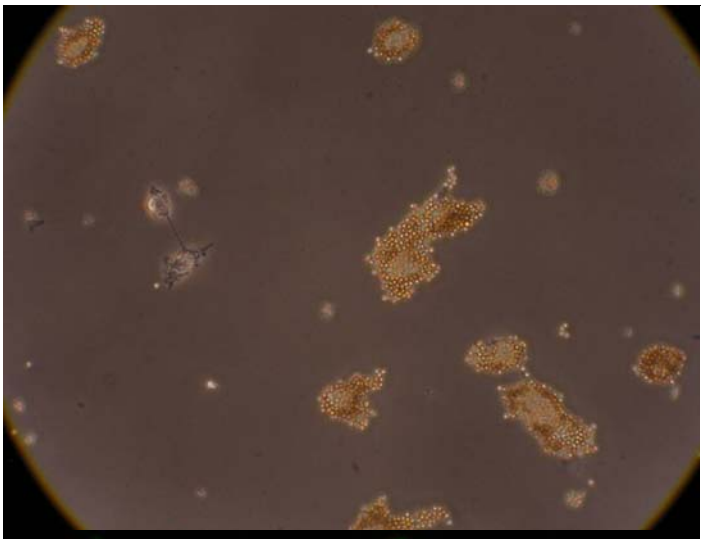

Figure 18a- COS-7cells transfected with the **glutamate to alanine** mutant binding ICAM-1 covered beads. This is a representative example of the type of view used for counting, and the amount of beads bound by the glutamate mutant.

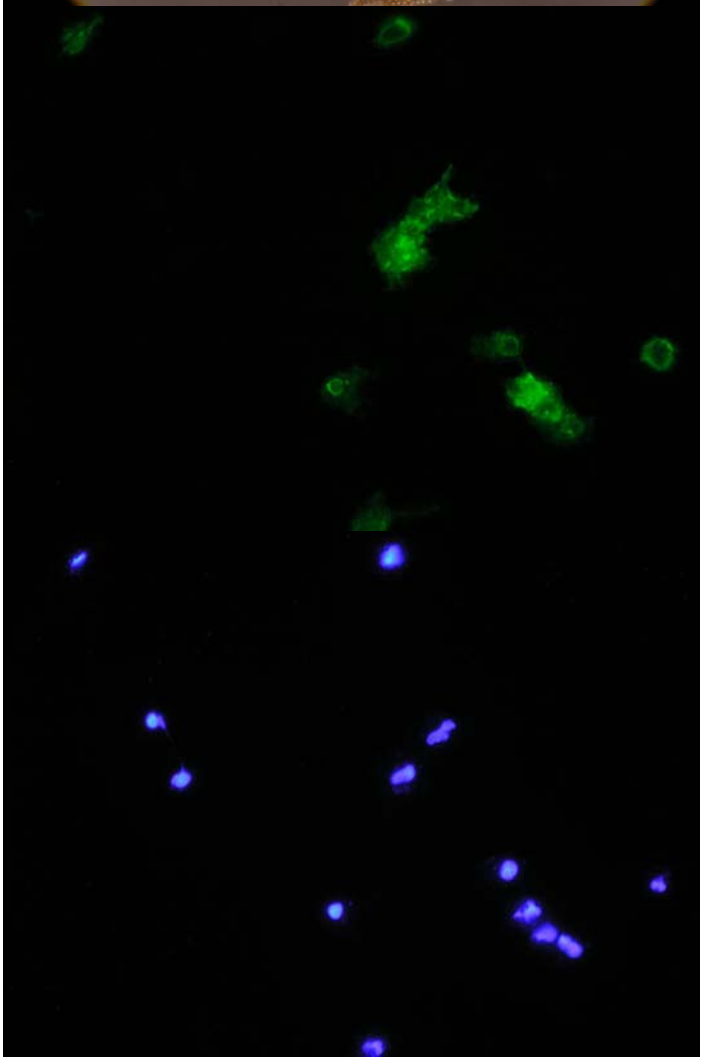

Figure 18b- Fluorescent image of the same transfected COS-7 cells seen in figure 18a. All of the green cells are expressing the construct, and binding ICAM-1 covered beads.

Figure 18c- Fluorescent image of the DAPI stained nuclei of the cells seen in figures 18a and 18b. Notice how this example skews the transfection efficiency as compared to the less constricted view in figure 14.

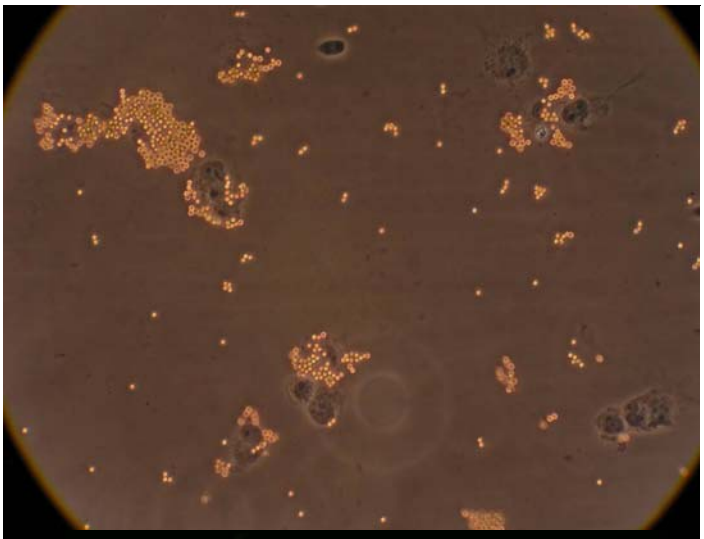

Figure 19a- COS-7cells transfected with the **lysine to alanine** mutant and binding ICAM-1 covered beads. This is a representative example of the type of view used for counting, and the amount of beads bound by the lysine mutant.

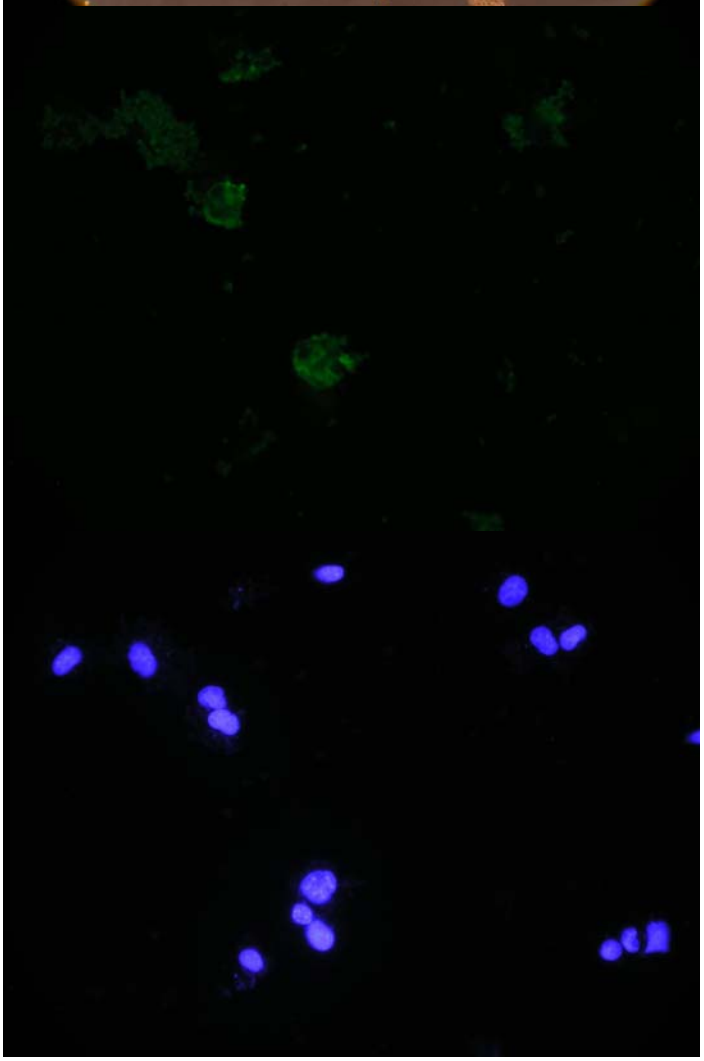

Figure 19b- Fluorescent image of the same transfected COS-7 cells seen in figure 19a. All of the green cells are expressing the construct, and binding ICAM-1 covered beads.

Figure 19c- Fluorescent image of the DAPI stained nuclei of the cells seen in figures 19a and 19b. Notice how this example skews the transfection efficiency as compared to the less constricted view in figure 15.

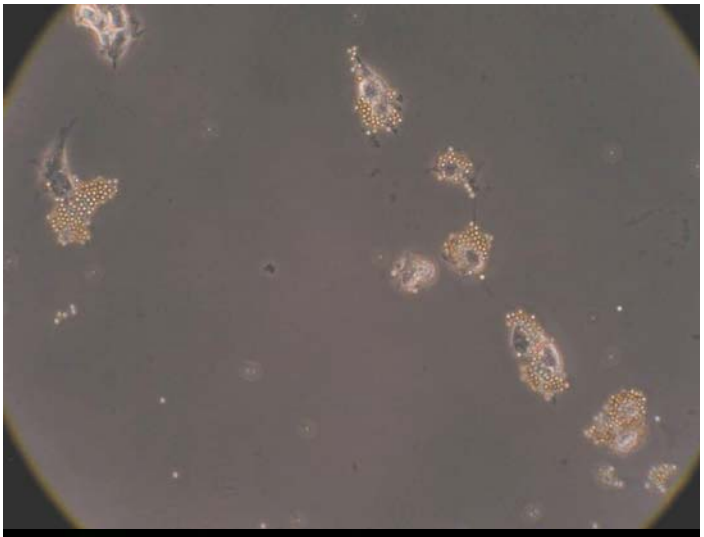

Figure 20a- COS-7cells transfected with the **threonine to alanine** mutant and binding ICAM-1 covered beads. This is a representative example of the type of view used for counting, and the amount of beads bound by the lysine mutant. Also, notice the lack of beads as compared to figures 17-19.

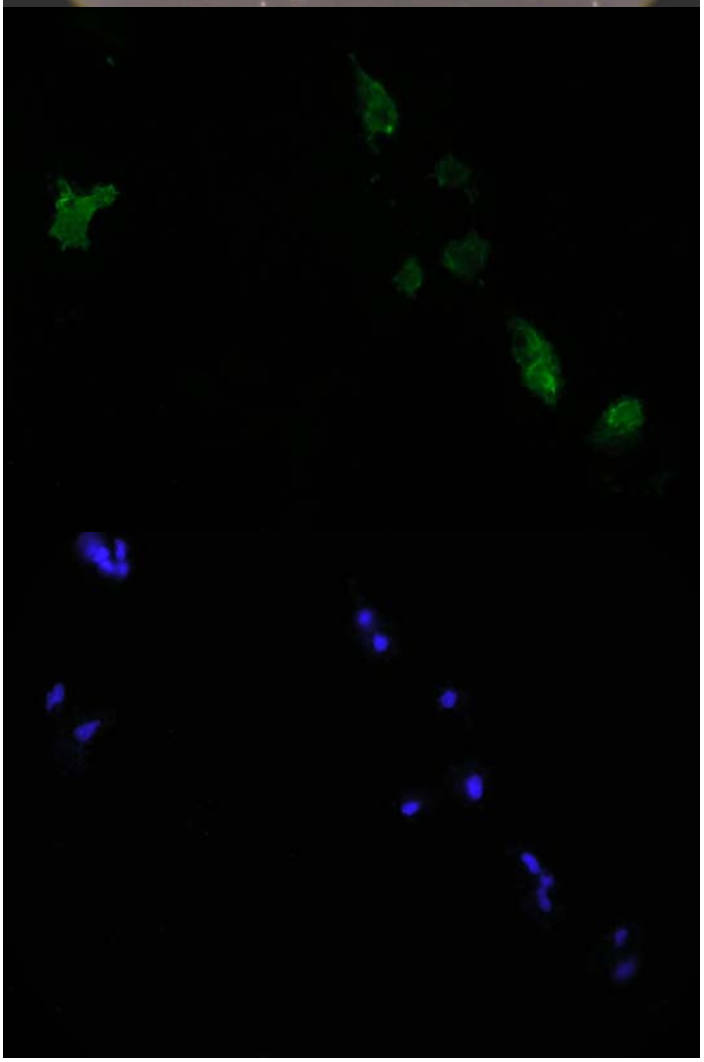

Figure 20b- Fluorescent image of the same transfected COS-7 cells seen in figure 20a. All of the green cells are expressing the construct, and binding ICAM-1 covered beads.

Figure 20c- Fluorescent image of the DAPI stained nuclei of the cells seen in figures 20a and 20b. Notice how this example skews the transfection efficiency as compared to the less constricted view in figure 16.

DISCUSSION

Model of DBL2β Region

The decision as to which amino acids would be substituted with alanine was based on several factors. I first looked at the overall proposed three dimensional structure of A4tres. In both the model of EBA-175 and A4tres there was a loop that protruded into the binding site region of the EBA-175 protein. The outer most part of this loop was made up of mostly polar amino acid residues, while the base of the loop varied in polarity and charge. The base of the loop was also one of the binding sites for glycan residue ligand. Due to the location of EBA-175 glycan binding site, I originally hypothesized that the base of the A4tres structure was the possible binding site for ICAM-1 and the polar amino acid loop merely existed to stabilize the protein in aqueous conditions.

Upon further inspection of the amino acids involved in glycan binding in the EBA-175 DBLβ domain, my initial assumptions began to change. There were several similarities between amino acids in the EBA-175 DBLβ region involved in glycan binding and the amino acids of A4tres that were predicted to be in the same area. The binding region of EBA-175 that overlapped with the A4tres structure contained 3 amino acid residues that interacted with the ligand: lysine, aspartate, and valine. Of these three, the aspartate and valine residues seemed to be somewhat conserved in PFEMP1 as A4tres, IT-ICAM, and FCRvarCSA all

contain these two amino acids at homologous positions. In general, residues that are conserved across many members of a family usually have either a structural or functional significance. The fact that these residues are conserved across not only the ICAM binding PfEMP1 (A4tres, IT-ICAM) but also in the non-ICAM binder FCRvarCSA suggests that these residues are structurally important, and not involved in binding.

Based on the deletion experiments performed by Springer et al. (2004), it is probable that amino acids near the conserved tryptophan (aa829) are important for binding. The EBA-175 glycan binding site is also near a conserved tryptophan. Therefore, it is possible that the equivalent region of A4tres is involved in binding ICAM-1 only utilizing different amino acids. In the proposed A4tres structure there is a lysine residue (aa831) that protruded into the same region as 3 residues involved in the EBA-175 binding site. Also, in the EBA-175 reaction sites lysine was often involved in binding glycans. I hypothesized that the lysine (aa831) could be involved in ionic interactions with ICAM-1 since the lysine (aa831) is positively charged and positioned near the binding site of EBA-175. If this assumption was accurate then substituting the lysine residue (aa831) with alanine would disrupt binding.

The glutamate residue (aa834) of A4tres is on the exact opposite side of the homologous EBA-175 binding region. In EBA-175 the homologous residue to the A4tres glutamate (aa834) did not appear to be involved in any of the other glycan binding reaction sites in EBA-175. The glutamate residue (aa834) is also

completely conserved among A4tres, IT-ICAM, and FCRvarCSA suggesting that it may have more structural importance rather than being part of a reaction site. Consequently, I hypothesized that if I substituted that glutamate residue (aa834) with alanine, ICAM-1 binding would not be changed. Moreover, if ICAM-1 binding was disrupted it might be due to a change in the overall structure of DBLβ domain rather than direct interference with the ICAM-1 binding site.

Tse et al. (2004) further characterized ICAM-1 by substituting alanine for residues in ICAM-1. While Tse et al. (2004) did not specifically look at the binding interactions between A4tres and ICAM-1, they did study IT-ICAM which is related to A4tres. Under static conditions, ICAM-1 binding was lessened when several nonpolar residues or the polar residues serine22 and cysteine21 were converted to alanine (figure 4). These results suggest that ICAM-1 may bind to IT-ICAM through either polar or nonpolar interactions. Assuming the same may be true for A4tres, I took a closer look at the outermost part of the polar loop.

In the EBA-175 DBLβ loop, two residues were involved in dimerization. The threonine residue at amino acid position 340 and the leucine residue at amino acid position 338 (Tolia et al., 2005). While A4tres is not a dimer, the homologous residues may still be involved in some other interactions. The EBA-175 residues align with a tyrosine and threonine residue (aa837) respectively. The threonine (aa837) juts into the aqueous surroundings at the very tip of the loop. At this position it would be possible for this residue to bind in a pocket on ICAM-1 through polar interactions.

Based on this view I chose the threonine residue for mutational analysis because it is a polar residue on the outermost portion of the loop that might be in contact with the ligand. Moreover, I hypothesized that it if I converted threonine (aa837) to alanine these polar interactions might not occur, disrupting binding of ICAM-1. For these reasons I chose threonine (aa837), lysine (aa831) and glutamate (aa834) to convert to alanine in order to better elucidate the binding interactions between ICAM-1 and A4tres.

Mutagenesis of Glutamate

When binding/immunofluorescence assays were performed on the glutamate (aa834) to alanine mutant, the average number of beads per cell was 95.4. This number is an increase from the 72.6 beads that were bound per cell for the control A4tres, suggesting that the glutamate to alanine mutant has enhanced binding. I believe this difference is significant, however it is also possible that ICAM-1 binding was unchanged as my ability to accurately count the number of beads on a cell is dependent on several factors. First, as the number of beads on a cell increases, my accuracy diminishes. Second, since cells are three dimensional structures, depth of field becomes an important factor in counting beads. Obviously cells that lie flat in one plane are easier to count than cells that are in four or more separate planes. Third, the arrangement of the beads on the cell is

important. It is more difficult to lose place in counting when beads are arranged irregularly as opposed to being a solid sheet.

Also, averages can be deceiving as the number of beads per cell varies considerably from cell to cell (appendix 2). For example, in the glutamate mutant the number of beads per cell ranges from 20-527, while in A4tres the number of beads per cell ranges from 7-173. This discrepancy in binding can be both attributed to natural variations in the assay, and variations in cell size. Clearly larger cells will bind more beads than smaller cells. As for variations in the assay, beads will undoubtedly be knocked off in the handling process. Also, the disruption of the beads during incubation and the amount of PfEMP1 being expressed in any given cell at the time of assay plays a large role in the number of beads bound.

In an attempt to limit the effect of these variations I set several guidelines in my counting procedure. First, I made sure to count cells that were towards the middle of the coverslip as opposed to the outskirts as the beads tended to be more equally distributed in the center. Second, I counted cells that were distributed on the coverslip in low densities. For practical reasons this was important because as the density of cells increased, it became harder to differentiate which cells were expressing the construct as well as which beads were attached to which cells. Third, I paid attention to the size of the cells as I counted. It was impossible to avoid variation in cell size, so I tried to count regions that had a similar fluctuation in cell size. In general I avoided areas that were comprised mostly of

tiny cells or enormous cells. As I was counting I also made the assumption that I wasn't counting the true number of beads on any given cell but that I would be wrong by the same proportion on all the cells I counted so it should not affect the overall results too greatly. Therefore, in general the results for these experiments should be taken more as guidelines than hard rules. In order to be more positive about the true nature of these interactions one would need to conduct additional experiments (see future experiments).

Although, assuming for a moment that these numbers correlate to the actual binding interactions between ICAM-1 and the DBL2β domain, there are possible explanations for this enhanced binding behavior. Based on the structure, it is not unlikely that ICAM-1 binding could be slightly sterically hindered by the presence of the large charged R-group on glutamate. The absence of glutamate (aa834) may allow ICAM-1 both easier access to the actual binding site and a tighter fit to the binding residues. Since extremely strong binding interactions are not necessarily an advantage for a protein, this may have evolved as a mechanism to decrease binding. Another possible explanation is that glutamate (aa834) plays an important role in maintaining the overall structure of the entire protein. Glutamate may form ionic interactions with a completely separate part of the protein possibly even the c2 domain. By converting it to alanine, the protein structure could have changed considerably, making the binding of ICAM-1 stronger.

Whether or not the glutamate (aa834) mutant has enhanced binding or is equal to A4tres, the results support my hypothesis that the glutamate residue (aa834) is not directly involved in binding.

Mutagenesis of Lysine

While the average number of beads per cell was greater for A4tres than for the alanine substituted lysine mutant (72.6 and 66.3 respectively), the difference is small enough that I believe the substitution had no effect on the protein's ability to bind ICAM-1. Considering all the factors that effect the average number of beads per cell (see Mutagenesis of Glutamate), a difference of 6.3 beads per cell is very small.

However, this result is interesting as it contradicts my original hypothesis that lysine (aa831) was involved in binding ICAM-1 and replacing lysine with alanine would decrease ICAM-1 binding. Lysine (aa831) was chosen to mutate because it was near the base of the loop, and protruded into the same region as the EBA-175 DBLβ binding site. Therefore, this result could be taken as possible evidence that the EBA-175 DBLβ binding site is not the same as the ICAM-1 binding site on the PfEMP1 DBL2β. This would further suggest that in PfEMP1 DBL2β domains the loop itself is involved in binding rather than its base. It is also possible that the binding site is at the base of the loop but that ICAM-1 binds in such a way that the lysine residue (aa831) has little effect.

Again, as in the glutamate mutant, this result only applies when looking at lysine singularly. If more residues where concurrently converted to alanine, a different result may be seen.

Mutagenesis of Threonine

The threonine mutant showed a marked decrease in ICAM-1 binding with an average of 42 beads per cell (A4tres- 72.6 beads per cell). The number of beads per cell ranged from 6-147, which is a similar range to the A4tres control. However, the decrease in binding is large enough that it can be observed even without counting the beads (figures 16 & 20). Consequently, even though this assay is not rigorously quantitative (see Mutagenesis of Glutamate), I am fairly confident that converting threonine (aa837) to alanine disrupts ICAM-1 binding.

Given this result, the question becomes the following: what mechanism is causing this change in ICAM-1 binding? A tantalizing idea is the possibility that threonine (aa837) is directly involved in hydrogen bond formation between ICAM-1 and the DBL2β domain. On the other hand, another idea that is very probable is that converting the polar threonine residue (aa837) to the more nonpolar alanine residue completely or partially deformed the loop. Since the threonine residue (aa837) is at the very tip of this polar loop, it is easy to imagine the loop inverting to a more thermodynamically stable position where the nonpolar residue isn't ordering the aqueous surroundings. However, the shape of

the loop may not change to a great extent, if at all, since alanine's R-group is only a single methyl group. Clearly, since the probable binding site is in the vicinity of the loop, any distortion of the loop may interfere with ICAM-1's ability to bind to the DBL2β domain.

Another proposal is that threonine (aa837) may be interacting with another part of the protein, perhaps the c2 domain. After all, the homologous residue in the EBA-175 DBLβ was involved in dimerization of the protein rather than ligand binding (Tolia et al., 2005). This could disrupt ICAM-1 binding if there are residues on another part of the protein that also bind ICAM-1 or if the other part of the protein stabilizes the binding site in the loop area.

Transfection Efficiencies

The transfection efficiencies reported in the results had a wide range from 32.9% to 87.7%, however this may be an overestimate of the actual transfection efficiencies. During the process of quantifying the cells, I not only kept in mind all the criteria listed previously for accuracy of my bead count estimates (see Mutagenesis of Glutamate), but looked for areas that showed a lot of green fluorescence since my goal was to count at least 50 green cells expressing the construct. Due to this my transfection efficiencies tend to be higher than expected. Since I didn't need to count beads for the FCRvarCSA construct, I looked at areas more randomly. Therefore, the transfection efficiencies for

FCRvarCSA are probably the closest to the actual transfection efficiency. Based on the results from FCRvarCSA and pictures from areas with high cell density (figures 12-15), I would estimate the actual transfection efficiency to range between 20 - 50%.

Standard Deviation

The standard deviations for the average number of beads per cell are fairly similar to each other, ranging from 20.6 to 40.2. The standard deviations are even more similar when comparing two clones from the same construct. The exception to both of these observations was the glutamate to alanine construct (clone 2) which was 86.1. These large numbers are reflective of the limitations of the quantitative aspect of the binding/immunofluorescence assays. The two lowest standard deviations 20.6 and 28.8 belonged to the threonine mutants (clones 1 and 2 respectively). These lower standard deviations are probably partially due to the fact that my accuracy in counting beads increases as the number of beads on a cell decreases. The high standard deviation in the glutamate mutant clone 2 can be traced to the fact that that preparation had a greater variability in cell size than the others. The standard deviations are similar to each other. Therefore, estimates for the average number of beads per cell for each construct can probably be compared to one another since they are subject to the same sources of error.

Also, if one calculates the percentage achieved by dividing the standard deviation of the average by the average number of beads per cell there is even a greater similarity between clones. The exceptions are again the glutamate clones. The glutamate clone 1 has the lowest percentage of 40%, while the glutamate clone 2 has the highest percentage of 88.9%. The percentage of the other clones ranges from 53.6 - 61.1%. The similarity between these percentages further suggests that the averages are valid.

CONCLUSION AND FUTURE EXPERIMENTS

Based on the results of the binding/immunofluorescence assay, we have more insight into the possible binding region of ICAM-1. The lysine residue (aa831) is most likely not involved in binding, while there is a possibility that converting the glutamate residue (aa834) to alanine produces a protein with enhanced ICAM-1 binding ability. Also, mutating threonine (aa837) to alanine caused a noticeable decrease in binding, suggesting that it either has binding interactions with ICAM-1 or that it is an important structural component of the protein. However, to have more definitive conclusions these experiments should be repeated several more times.

This same assay could be modified in two separate ways to produce more quantitative results. First, by titrating the concentration of ICAM-1 or number of beads used one could produce more obvious results. By gradually lowering the concentration of ICAM-1used in the binding/immunofluorescence assay, a complete loss or more exaggerated loss of binding may be seen in the threonine mutant. These results then could be compared to the A4tres control at the same concentration of ICAM-1. If at this concentration A4tres still bound ICAM-1 and the threonine mutant did not, more positive conclusions could be made. Likewise, the glutamate mutant may show a more marked increase in binding or possibly continue to bind ICAM-1 at concentrations where A4tres will not.

A second method that may produce more quantitative results would be to attach a fluorescent antibody to ICAM-1 rather than magnetic beads. Using a different color antibody than the Alexa488 used to label the construct would allow one to more accurately quantify the results. The amount of overlap from the two different antibodies could be measured using flow cytometry. In flow cytometry the cells would be counted individually and the intensity of fluorescence from each recorded. This method would eliminate all of the error associated with counting beads.

Since A4tres has been modified by treating IE's with trypsin (Smith, Craig et al., 2000), the ICAM-1 binding properties of A4tres are not naturally seen in untreated A4tres-expressing *Plasmodium falciparum* parasites. However, IT-ICAM is unmodified and binds ICAM-1 in IE's. Due to this, it might be more appropriate to continue these experiments using IT-ICAM as this PfEMP1 may be more applicable to the formation of a vaccine or drug. However, I would expect similar results in both A4tres and IT-ICAM as they have very similar sequences in the proposed binding region.

Other future experiments would be to convert other amino acid residues in this possible binding region to alanine and possibly make double substitutions. For example I would like to change the tyrosine and serine in A4tres to alanine. The tyrosine and serine residues are next to the region involved in glycan binding in the EBA-175 DBLβ domain, and are conserved in both IT-ICAM and A4tres but not in FCRvarCSA suggesting that they maybe involved in ICAM-1 binding.

Furthermore, since the c2 domain has been implicated in binding ICAM-1 along with the DBL2β domain (Springer et al., 2004, Smith et al., 2001) site-specific mutagenesis along with the binding/immunofluorescence assays could be used to better elucidate the structure, binding interactions and relationship of the c2 domain with the DBL2β domain. However, there is no crystal structure of the c2 domain to use for homologous modeling. Therefore, it may be difficult to choose residues in the c2 domain to switch to alanine.

The main drawback of using site-specific mutagenesis along with the binding/ immunofluorescence assays to characterize the binding region of a protein lies in the inability of the assays to distinguish loss of binding due to a change in amino acids that interact with the ligand and loss of binding due to a structural change in the protein. While using site specific mutagenesis to convert a single amino acid to alanine is less likely to impact the overall structure of the protein than using deletions, it is still a possibility. The best way to truly characterize the binding interactions between the DBL2β domain and ICAM-1 would be to solve the crystal structure of the DBL2β domain interacting with its ligand.

This study has further characterized the possible binding region of A4tres, and has helped to better understand the residues and mechanisms involved in ICAM-1. Additional characterization of the ICAM-1/ PfEPM1 binding interactions could aid in the development of drugs that prevent the binding of IE's to ICAM-1 which could decrease the severity of the symptoms of malaria. In time a vaccination against malaria may be achieved.

APPENDIX

Appendix A: Tables of the cell counts used to quantify the results

Bead Counts for Each Alanine Substituted Amino Acid						
	E1	E2	T1	T2	K3	K4
# DAP1	63	114	65	91	100	74
# Green	52	55	57	54	51	53
# Green w/ Beads	52	55	56	52	51	53
# Beads Each Cell:						
1	67	243	51	62	26	41
2	100	125	6	63	59	77
3	76	527	21	65	41	139
4	81	62	61	79	160	91
5	60	62	71	51	60	19
6	109	63	34	34	48	24
7	98	63	20	61	26	98
8	66	189	44	52	59	58
9	58	139	29	42	53	59
10	100	111	27	60	79	128
11	84	111	73	22	47	109
12	144	164	20	16	58	64
13	100	38	20	8	34	95
14	61	118	21	30	57	53
15	80	155	40	56	169	8
16	100	156	8	20	43	69
17	56	350	26	107	92	43
18	55	70	27	92	151	58
19	105	65	37	57	103	64
20	150	92	38	147	115	140
21	90	59	76	55	132	25
22	140	46	28	83	46	51
23	95	47	11	83	31	23
24	81	47	27	120	101	11
25	252	162	44	65	35	30
26	111	113	86	57	130	31
27	38	98	64	54	128	28
28	50	103	20	64	12	39
29	174	20	20	34	50	40
30	127	20	20	20	91	83

31	85	21	20	20	105	32
32	90	21	21	21	16	84
33	170	46	21	33	93	76
34	107	46	47	50	76	15
35	67	46	90	50	120	123
36	88	46	33	50	59	89
37	95	42	43	50	33	43
38	80	43	44	53	27	8
39	85	123	21	73	38	66
40	85	45	35	22	100	51
41	118	176	33	23	58	50
42	90	27	7	6	50	110
43	60	27	7	6	50	139
44	64	51	5	36	71	145
45	89	61	9	36	130	107
46	72	60	8	37	19	46
47	49	40	9	13	27	47
48	118	41	61	44	49	40
49	48	156	26	52	52	75
50	48	163	37	83	26	82
51	120	68	38	28	38	100
52	147	68	38	73		13
53		145	46			40
54		73	47			105
55		73	47			
Average # of Bead/Cell	93.90385	96.83636	33.87273	50.34615	68.09804	64.51852
Total	95		42		66.3	

Bead Counts for A4tres and FCR Controls				
	A4tres	A4tres	FCR	FCR
# DAP1	112	112	111	136
# Green	51	51	57	54
# Green w/ Beads	51	51	0	0
# Beads Each Cell:				
1	83	24		
2	83	40		
3	124	21		
4	63	7		
5	49	17		
6	50	54		
7	44	111		
8	44	74		
9	50	80		
10	66	93		
11	72	94		
12	39	94		
13	40	64		
14	68	66		
15	159	13		
16	45	18		
17	48	46		
18	49	74		
19	17	13		
20	129	103		
21	173	50		
22	111	14		
23	29	116		
24	21	65		
25	26	169		
26	6	31		
27	90	31		
28	66	29		
29	104	108		
30	25	154		
31	37	76		
32	38	77		
33	145	77		
34	25	132		
35	80	54		
36	76	84		
37	61	84		
38	107	84		
39	107	148		

40	110	94		
41	98	53		
42	84	52		
43	100	46		
44	91	27		
45	92	79		
46	136	59		
47	74	60		
48	59	78		
49	145	78		
50	146	78		
51	146	78		
52				
Average # of Bead/Cell	77.05882	68.05882		
	72.6			

Appendix B: Structure of 20 Amino Acids

Pictures from http://en.wikipedia.org/wiki/Amino_acid

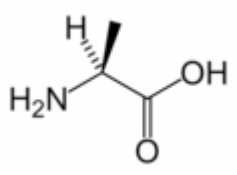

Alanine (Ala / A)

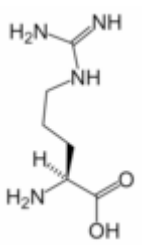

Arginine (Arg / R)

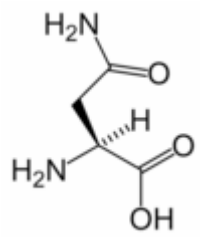

Asparagine (Asn / N)

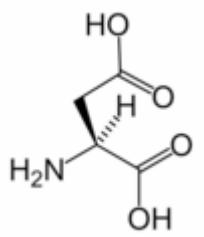

Aspartic acid (Asp / D)

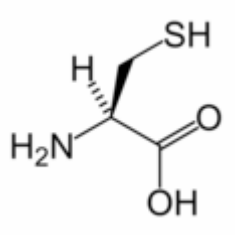

Cysteine (Cys / C)

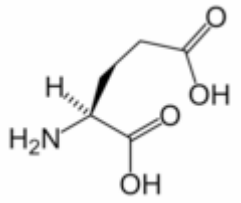

Glutamic Acid (Glu / E)

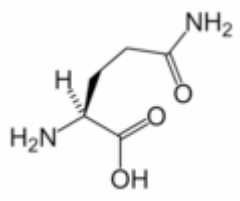

Glutamine (Gln / Q)

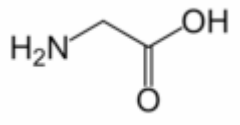

Glycine (Gly / G)

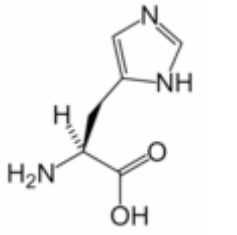

Histidine (His / H)

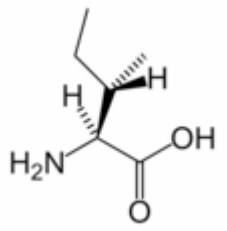

Isoleucine (Ile / I)

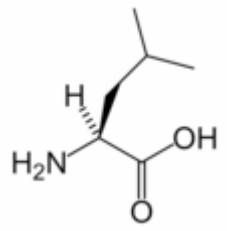

Leucine (Leu / L)

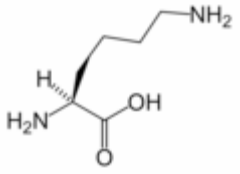

Lysine (Lys / K)

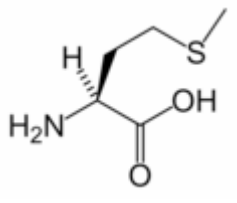

Methionine (Met / M)

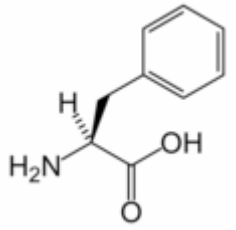

Phenylalanine (Phe / F)

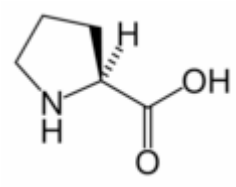

Proline (Pro / P)

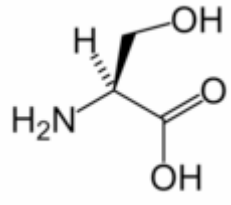

Serine (Ser / S)

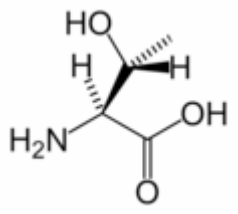

Threonine (Thr / T)

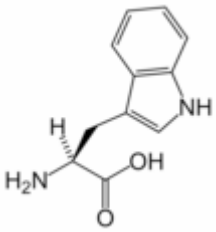

Tryptophan (Trp / W)

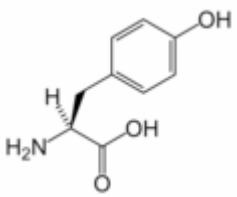

Tyrosine (Tyr / Y)

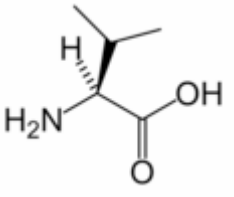

Valine (Val / V)

Appendix C: Commonly used abbreviations and names

A4- ICAM-1 binding line of IT 4/25/5

A4tres- line of IT 4/25/5 that binds ICAM-1 used in this study. A line derived from A4 that has been treated by trypsin.

DBL2βc2- tandem domains of PfEMP1 known to bind ICAM-1

EBA-175- Erythrocyte Binding Antigen 175- invasion protein that contains a DBLβ domain.

FCRvarCSA- line of IT 4/25/5 that does not bind ICAM-1

IE's- erythrocytes infected with *Plasmodium*

IT 4/425/5- Strain of *Plasmodium falciparum* (strain is a genetic variant)

IT-ICAM- another ICAM-1 binding line of IT 4/25/5

PfEMP1- *Plasmodium falciparum* Erythrocyte Membrane Protein 1- variant antigen placed on the surface of IE's

LITERATURE CITED

Adams JH, Sim BKL, Dolan SA, Fang X, Kaslow DC, Miller LH. 1992. A family of erythrocyte binding proteins of malaria parasites. *Proc. Natl. Acad. Sci. USA.* **89**(15): 7085-7089.

Barnwell JW, Asch AS, Nachman RL, Yamaya M, Aikawa M, Ingravallo P. 1989. A human 88-kD membrane glycoprotein (CD36) functions *in vitro* as a receptor for a cytoadherence ligand on *Plasmodium falciparum*-infected erythrocytes. *J. Clin. Ivest.* **84**: 765-72.

Baruch D.I, Ma XC, Singh HB, Bi X, Pasloske BL, Howard RJ. 1997. Identification of a region of PfEMP1 that mediates adherence of *Plasmodium falciparum* infected erythrocytes to CD36: conserved function with variant sequence. *Blood*. **90**: 3766-3775.

Buffet PA, Gamain B, Scheidig C, Baruch D, Smith JD, Hernandez-Rivas R, Pouvelle B, Oishi S, Fujii N, Fusai T, Parzy D, Miller LH, Gysin J, Scherf A. 1999. *Plasmodium falciparum* domain mediating adhesion to chondroitin sulfate A: a receptor for human placental infection. *Proc. Natl. Acad. Sci. USA*. **96**(22): 12743-8.

CDC- Center for Disease Control and Prevention. 2004. Malaria topic home. http://www.cdc.gov/malaria/ (accessed 2005)

Chattopadhyay R, Taneja T, Chakrabarti K, Pillai CR, Chitnis CE. 2003. Molecular analysis of the cytoadherence phenotype of a *Plasmodium falciparum* field isolate that binds intercellular adhesion molecule-1. *Mol. Biochem. Parasitol*. **133**(2): 255-265.

Chakravorty SJ, Craig A. 2005. The role of ICAM-1 in *Plasmodium falciparum* cytoadherence. *European J. Cell Biol*. **84**: 15-27.

Clackson T, Wells JA. 1995. A hot spot of binding energy in a hormone-receptor interface. *Science*. **267**: 383-386.

Fernandez-Reyes D, Craig AG, Kyes SA, Peshu N, Snow RW, Berendt AR, Marsh K, Newbold CI. 1997. A high frequency African coding polymorphism in the N-terminal domain of ICAM-1 predisposing to cerebral malaria in Kenya. *Hum. Mol. Genet.* **6**(8): 1357-60.

Fried M, Duffy PE. 1996. Adherence of *Plasmodium falciparum* to chondroitin sulfate A in the human placenta. *Science*. **272**(5267): 1502-04.

Fried M, Nosten F, Brockman A, Brabin BJ, Duffy PE. 1998. Maternal antibodies block malaria. *Nature*. **395**(6705): 851-2.

Good MF. 2001. Towards a blood-stage vaccine for malaria: are we following all the leads?. *Nature Reviews*. **1**: 117-125.

Good MF, Stanisic D, Xu H, Elliot S, Wykes M. 2004. Immunological challenge to developing a vaccine to the blood stages of malaria parasites. *Immunological Reviews*. **201**: 254- 267.

Greenwalt DE, Lipsky RH, Ockenhouse CF, Ikeda H, Tandon NN, Jamieson GA. 1992. Membrane glycoprotein CD36: a review of its roles in adherence, signal transduction, and transfusion medicine. *Blood*. **80**(5): 1105-15.

Guex N, Peitsch MC. 1997 SWISS-MODEL and the Swiss-PdbViewer: an environment for comparative protein modeling. *Electrophoresis* **18**:2714-2723.

Horrocks P, Pinches R, Christodoulou Z, Kyes SA, Newbold CI. 2004. Variable *var* transition rates underlie antigenic variation in malaria. *Proc. Natl. Acad. Sci. USA.* **101**(30): 11129-34.

Howell DP-G, Samudrala R, Smith JD. 2006. Disguising itself – insights into *Plasmodium falciparum* binding and immune evasion from the DBL crystal structure. *Mol Biochem Parasitol*. In press.

Kraemer SM, Smith JD. 2003. Evidence for the importance of genetic structuring to the structural and functional specialization of the *Plasmodium falciparum var* gene family. *Mol. Microbiol*. **50**(5): 1527-38.

Kyes S, Horrocks P, Newbold C. 2001. Antigenic variation at the infected red cell surface in malaria. *Annual Review Microbiol*. **55**: 673-707.

Miller LH, Baruch DI, Marsh K, Doumbo O. 2002. The pathogenic basis of malaria. *Nature*. **415**: 673-679.

Newbold C, Warn P, Black G, Berendt A, Craig A, Snow B, Msobo M, Peshu N, Marsh K. 1997. Receptor-specific adhesion and clinical disease in *Plasmodium falciparum*. *J. Trop. Med. Hygiene*. **57**: 389-98.

Ockenhouse CF, Tandon NN, Magowan C, Jamieson GA, Chulay J. 1989. Identification of a platelet membrane glycoprotein as a falciparum malaria sequestration receptor. *Science.* **243**(4897): 1469-71.

Piela-Smith TH, Aneiro L, Korn JH. 1991. Binding of human rhinovirus and T cells to the intercellular adhesion molecule-1 on human fibroblasts. Discordance between effects of IL-1 and IFN-gamma. *J. Immunol*. **147**(6): 1831-6.

Pongponratin E, Riganti M, Punpoowong B, Aikawa M. 1991. Microvascular sequestration of parasitized erythrocytes in human falciparum malaria: a pathological study. *Am. J. Trop. Med. Hyg.* **44**: 168-175.

Rogerson SJ, Chaiyaroj SC, Ng K, Reeder JC, Brown GV. 1995. Chondroitin sulfate A is a cell surface receptor for *Plasmodium falciparum*–infected erythrocytes. *J. Exp. Med*. **182**:15–20.

Rutherford K, Parkhill J, Crook J, Horsnell T, Rice P, Rajandream MA and Barrell B. 2000. Artemis: sequence visualization and annotation. *Bioinformatics.* **16**(10): 944-945.

Sachs JD. 2002. A new global effort to control malaria. *Science*. **298**(5591):122-4.

Singh SK, Hora R, Belrhali H, Chitnis CE, Sharma A. 2006. Structural basis for Duffy recognition by the malaria parasite Duffy-binding-like domain. *Nature*. **439**: 741-744.

Smith JD, Kyes S, Craig AG, Fagen T, Hudson-Taylor D, Miller LH, Baruch DI, Newbold CI. 1998. Analysis of adhesive domains from the A4var *Plasmodium falciparum* erythrocyte membrane protein-1 identifies a CD36 binding domain. *Mol. Biochem. Parasitol*. **97**: 133-48.

Smith JD, Craig AG, Kriek N, Hudson-Taylor D, Kyes S, Fagen T, Pinches R, Baruch DI, Newbold C, Miller LH. 2000. Identification of a *Plasmodium falciparum* intercellular adhesion molecule-1 binding domain: a parasite adhesion trait implicated in cerebral malaria. *Proc. Natl. Acad. Sci. USA.* **97**(4): 1766-71.

Smith JD, Subramanian G, Gamain B, Baruch DI, Miller LH. 2000. Classification of adhesive domains in the *Plasmodium falciparum* erythrocyte membrane protein 1 family. *Mol. Biochem. Parasitol*. **110**: 293-310.

Smith JD, Gamain B, Baruch DI, Kyes S. 2001. Decoding the language of var genes and *Plasmodium falciparum* sequestration. *TRENDS Parasitol*. **17**(11): 538-45.

Smith JD, Craig A. 2004. The surface of the *Plasmodium falciparum*–infected erythrocyte. Chapter 12: Malaria Parasites: Genome and Molecular Biology. Horizon Press.

Snow RW, Craig M, Deichmann U, Marsh K. 1999. Estimating mortality, morbidity and disability due to malaria among Africa's non-pregnant population. *Bull. WHO*. **77**: 624-40.

Snow RW, Guerra CA, Noor AM, Myint HY, Hay SI. 2005. The global distribution of clinical episodes of *Plasmodium falciparum* malaria. *Nature*. **434**: 214-217.

Springer AL, Smith LM, MacKay DQ, Nelson SO, Smith JD. 2004. Functional interdependence of the DBLβ domain and the c2 region for binding of the *Plasmodium falciparum* variant antigen to ICAM-1. *Mol. Biochem. Parasitol*. **137**: 55-64.

Stolpe AV, Saag PT. 1996. Intercellular adhesion molecule - 1. *J. Mol. Med*. **74**: 13-33.

Su XZ, Heatwole VM, Wertheimer SP, Guinet F, Herrfeldt JA, Peterson DS, Ravetch JA, Wellems TE. 1995. The large diverse gene family *var* encodes proteins involved in cytoadherence and antigenic variation of *Plasmodium falciparum*-infected erythrocytes. *Cell.* **82**(1): 89-100.

Tse MT, Chakrabarti K, Gray C, Chitnis CE, Craig A. 2004. Divergent binging sites on the intercellular adhesion molecule-1 (ICAM-1) for variant *Plasmodium falciparum* isolates. *Mol. Microbiol*. **51**(4): 1039 – 49.

Tolia NH, Enemark EJ, Sim BKL, Joshua-Tor L. 2005. Structural basis for the EBA-175 erythrocyte invasion pathway of the malaria parasite *Plasmodium falciparum*. *Cell*. **122**: 183-93.

Turner GD, Morrison H, Jones M, Davis TM, Looareesuwan S, Buley ID, Gatter KC, Newbold CI, Pukritayakamee S, Nagachinta B. 1994. An immunohistochemical study of the pathology of fatal malaria. Evidence for widespread endothelial activation and a potential role for intercellular adhesion molecule-1 in cerebral sequestration. *Am. J. Pathol*. **145**(5): 1057-69.

Turner GD, Ly VC, Nguyen TH, Tran TH, Nguyen HP, Bethell D, Wyllie S, Louwrier K, Fox SB, Gatter KC, Day NP, Tran TH, White NJ, Berendt AR. 1998. Systemic endothelial activation occurs in both mild and severe malaria.

Correlating dermal microvascular endothelial cell phenotype and soluble cell adhesion molecules with disease severity. *Am. J. Pathol*. **152**(6): 1477-87.

Waters AP. 2005. *Plasmodium*'s sticky fingers. *Cell*. **122**(2): 149-51.

Weatherall DJ, Miller LH, Baruch DI, Marsh K, Doumbo OK, Casals-Pascual C, Roberts DJ. 2002. Malaria and the red cell. *Hematology*. 2002: 35-57.